https://doi.org/10.5194/egusphere-2025-814
Preprint. Discussion started: 11 April 2025

Revisiting the geodynamic model for the Mako greenstone belt: new evidence for a Paleoproterozoic oceanic plateau in the West African Craton.

Ibrahima Labou[1], German Velásquez[2,3], Mathieu Benoit[3], Lenka Baratoux[3,4,5], Didier Béziat[3], Pierre Debat[3], Papa Moussa Ndiaye[6]

[1] National Superior School of Mines and Geology, Cheikh Anta Diop University, Dakar, Senegal
[2] Instituto de Geología Económica Aplicada, Universidad de Concepción, casilla 160-C, Concepción, 4070386, Chile
[3] GET-OMP, University of Toulouse III Paul Sabatier, CNRS - IRD - UPS; 14 Av. Edouard Belin, Toulouse 31400, France
[4] Fundamental Institute of Black Africa (IFAN), Cheikh Anta Diop, Dakar, Senegal
[5] Université Félix Houphouët-Boigny (UFHB), Abidjan-Cocody, UFR STRM, 22 BP 582 Abidjan 22, Côte d'Ivoire
[6] Department of Geology, Faculty of Science and Technology, Cheikh Anta Diop University, Dakar, Senegal

Correspondence to: Ibrahima Labou (ibrahima1.labou@ucad.edu.sn)

Abstract: Geochemical and isotopic data from the Paleoproterozoic greenstone belt of Mako (Eastern Senegal) provide evidence for the existence of two tholeiitic and one calc-alkaline series. Tholeiitic series are composed of ultramafic and mafic rocks. Tholeiites 1 are characterized by flat Light Rare Earth Elements (LREE) and Middle Rare Earth Elements (MREE) patterns and by initial isotopic compositions of $^{87}Sr/^{86}Sr$ (2.1 Ga) from 0.70083 to 0.70368 and εNd (2.1 Ga) from +1.55 to +5.90 (except sample IL49). Tholeiites 2 are characterized by a more enriched LREE and MREE pattern, and by initial isotopic compositions $^{87}Sr/^{86}Sr$ (2.1 Ga) from 0.7009 to 0.70263 and εNd (2.1 Ga) from +2.14 to +7.35. In addition tholeiites 2 show a slightly negative Nb anomaly, while the tholeiites 1 have no Nb anomaly. Calc-alkaline rocks are characterized by more enriched LREE and MREE patterns and more depleted Heavy Rare Earth Elements (HREE), indicating more pronounced general LREE/HREE fractionation; they have a more pronounced negative Nb and Ti anomalies and initial isotopic signatures of $^{87}Sr/^{86}Sr$ (2.1 Ga) from 0.7009 to 0.70618 and εNd (2.1 Ga) from +3.12 to +6.40. Comparison of geochemical and isotopic data of the three magmatic series with those of other Paleoproterozoic domains of the West African Craton and juvenile volcanic rocks leads us to propose an evolutive model for the Mako series comprising an initial emplacement of an oceanic plateau, in which the first tholeiitic series was generated, followed by a subduction process that triggers the contamination of the mantle plume source and the generation of the second tholeiitic series at the earliest stages of the arc built; and ending with the maturation of an island arc and the calc-alkaline series emplacement, which has a chemical signature indicating that the source region was likely a metasomatized mantle probably mixed with some plume mantle source.

Keywords: Paleoproterozoic; West African Craton; Geochemistry; Sr/Nd isotopes; Oceanic plateau; Island arc.

1 Introduction

The greenstone belts, a volcanic-dominated submarine supracrustal assemblage found in all the Archean and Paleoproterozoic cratons, are characterized by two types of volcanic suites: 1) a komatiite-tholeiitic basaltic suite, and 2) a tholeiitic to calc-alkaline basalt-felsic bimodal suite, which can be associated with granitoid rocks (Condie, 1994). The difference in their geochemical affinities implies that these suites have different sources for the primary magma and are associated with different tectonic settings. A consensus has been reached for the petrogenetic model for the calc-alkaline series, which are interpreted to be formed in an arc context, associated with a subduction tectonic setting (e.g., Feybesse and Milési, 1994; Ama-Salah et al. 1996; Polat and Kerrich, 2002; Hollings and Kerrich, 2004; Grenholm et al., 2019; Hayman et al., 2023). On the other hand, the context of formation and evolution of the tholeiitic series is still under discussion and several geodynamic settings are still proposed. According to Furnes et al. (2015), the Precambrian tholeiitic series (basalts, gabbros and ultramafic rocks) can be grouped into two major series: i) subduction-related ophiolites (representing up to 85 % of the greenstone sequences in the world), which are generated in back arc to forearc tectonic environments, and ii) subduction-unrelated greenstone sequences, which have different origins, including tectonic settings from the oceanic basin evolution, through continental rifting, seafloor spreading, to plume magmatism. The great variety of geodynamic contexts considered for the interpretation of the series must be due to the coexistence of series formed in different geodynamic contexts and associated by collages (e.g., the Archean greenstone belt from Greenland, Polat et al., 1998). Similar petrogenetic models can be drawn for the Paleoproterozoic formations of the WAC, where two generations of volcanism, tholeiitic and calc-alkaline have been described (Abouchami et al., 1990; Boher et al., 1992; Sylvester et Attoh, 1992; Ama Salah et al., 1996; Baratoux et al., 2011 and references therein). The tholeiitic series are essentially composed of basalts and gabbros and, in some area, of rare and small slices of ultramafic (UM) rocks (see references in Labou et al., 2020). Ultramafic rocks are interpreted as cumulates of the tholeiitic series (Ouedraogo, 1985; Dia, 1988; Ngom, 1995; Ngom et al., 1998, 2010; Pouclet et al., 2006; Sangaré, 2008; Cissokho, 2010; Dabo et al., 2017; Labou et al., 2020), or genetically related to the calc-alkaline series (Béziat et al., 2000) or as the testimony of an ophiolitic supra-subduction environment (Attoh et al., 2006; Dabo et al., 2017; Dampare et al., 2019).

For the crustal growth of the tholeiitic series in the WAC, several models have been proposed: i) an intracontinental rift setting (Ratomaharo et al., 1988 in Burkina Faso; Alric, 1990 in Ivory Coast; Leube et al., 1990 in Ghana); ii) an oceanic plateau environment (Abouchami et al., 1990; Boher et al, 1992, Lompo, 2009 for the whole WAC; Pouclet et al., 1996, 2006, in Ivory Coast; Cissokho, 2010; Ngom et al., 2010 in Senegal; Agra et al., 2023 in Ghana); iii) a mid-ocean rift (MORB) (Zonou, 1987 in Burkina Faso; Ngom, 1995; Ngom et al., 2007; Theveniaut et al., 2010 in Senegal); iv) an intra-oceanic volcanic arc (Ama Salah et al., 1996 in Niger; Dia, 1988; Dia et al., 1997; Diallo, 2001; Pawlig et al., 2006 in Senegal; Béziat et al, 2000 in Burkina Faso; Sangaré, 2008 in Mali; Baratoux et al., 2011 in Burkina Faso) or v) in a back-arc context (Sylvester and Attoh, 1992; Attoh et al., 2006; Dampare et al., 2008, 2009 in Ghana). In addition, Attoh et al. (2006) and Dampare et al. (2019) in Ashanti, Ghana and Bassot (1966) and Dabo et al. (2017) in Mako, Senegal, have proposed an ophiolitic supra-subduction zone as tectonic setting for the volcanic rock formation.

The aim of this study is to revisit the tectonomagmatic evolution for a typical Paleoproterozoic greenstone belt in the WAC, taking as the study-case the Mako greenstone belt, located in eastern Senegal. We present new petrographic, mineralogical, and geochemical data, for the ultramafic and mafic suites of the Mako belt including whole-rock and "in-situ" mineral analyses, including major, trace elements and isotopic determinations from whole-rock analysis. The data are discussed: 1) to define the geochemical characteristics of the different volcanic suites recognized in the belt; 2) to

https://doi.org/10.5194/egusphere-2025-814
Preprint. Discussion started: 11 April 2025

evaluate the tectonic setting and mantle source for these rocks; 3) to discuss an evolutive model for the Mako greenstone belt in relation to those proposed for other Paleoproterozoic greenstone belts in the WAC.

2 Geological setting

2.1 West African Craton

The West African Craton (WAC) comprises mainly three separated domains (Bessoles, 1977) (**Fig. 1**): (i) the northern Reguibat Shield constituted by Archean (3.0 – 2.7 Ga) and Palaeoproterozoic series (2.3 – 1.9 Ga); (ii) the southern Leo-Man Shield consisting of the Archean formations of the Kenema-Man domain and the Paleoproterozoic formations of the Baoule-Mossi domain; (iii) the Kedougou and Kayes inliers only represented by Paleoproterozoic terrains. The Paleoproterozoic formations named Birimian (Kitson, 1928; Junner, 1954) correspond to narrow linear to arcuate volcanic greenstone belts and wider sedimentary units, which accreted around 2.0 Ga (Bonhomme, 1962) during the Eburnean orogeny. This orogeny is characterized by the emplacement of huge volumes of granitoids (Doumbia et al., 1998; Gasquet et al., 2003; Dioh et al., 2006; de Kock et al., 2011; Parra-Avila et al., 2017). The Birimian greenstone belts are constituted by two major series (Abouchami et al., 1990; Boher et al., 1992; Sylvester and Attoh, 1992): (i) a tholeiitic series comprising basalts, gabbros and rare UM bodies (dunites, harzburgites, lherzolites, wehrlites; Bassot, 1966; Dia, 1988; Ngom, 1995; Ngom et al., 1998; Loh et al., 1999; Béziat et al., 2000; Castaing et al., 2003; Attoh et al., 2006; Pouclet et al., 2006; Sangaré, 2008; Cissokho, 2010; Ngom et al., 2010; Dabo et al., 2017; Dampare et al., 2019; Labou et al., 2020); (ii) a calc-alkaline series comprising an ultramafic to differenciated suite (dunites, wehrlites, gabbros, basalts, andesites, dacites, rhyolites; Béziat et al., 2000; Labou et al., 2020) cross-cutting the tholeitic formations and the metasedimentary formations. Greenstone belts and sedimentary basins were subjected to a widespread greenschist-facies metamorphism (Bessoles, 1977) although high pressure-low temperature (HP-LT) metamorphism has been also reported (Debat et al., 2003; Pitra et al., 2010; Ganne et al., 2012, 2014; Block et al., 2015, 2016; Koffi et al., 2023).

https://doi.org/10.5194/egusphere-2025-814
Preprint. Discussion started: 11 April 2025

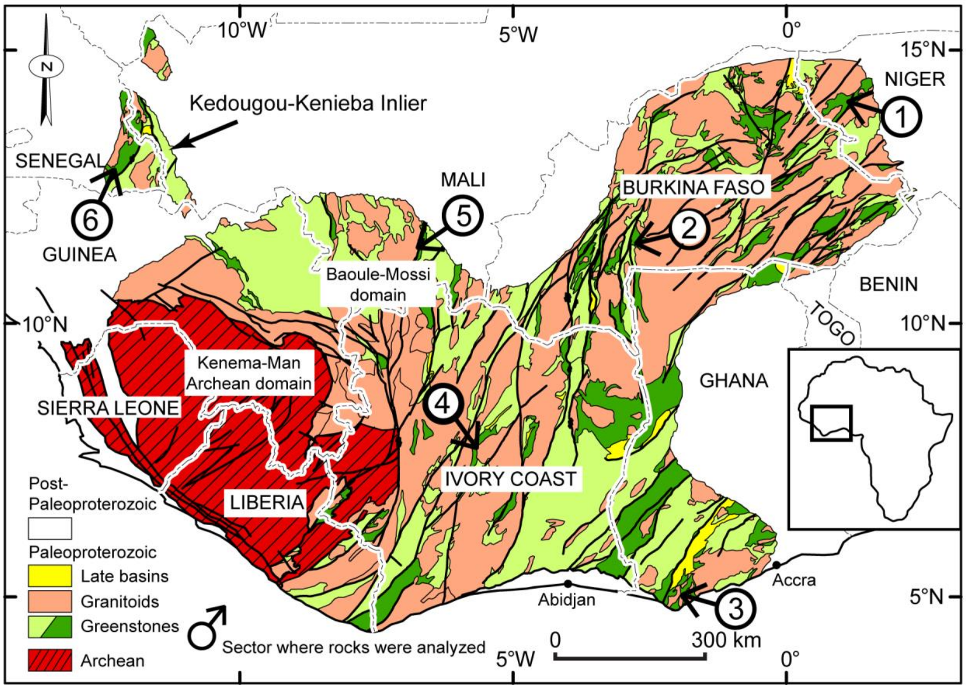

Figure 1: Geological map of the WAC (modified from Milesi et al., 2004 and Thieblemont et al., 2016) showing the sector where greenstone belts have been studied. Zone 1: Liptako belt in Niger (Abouchami et al., 1990; Ama Salah et al., 1996); Zone 2: Boromo and Hounde belts in Burkina Faso (Zonou, 1987; Abouchami et al., 1990; Béziat et al., 2000; Baratoux et al., 2011); Zone 3: Dixcove and Ashanti belts in Ghana (Leube et al., 1990; Sylvester et Attoh, 1992; Attoh et al., 2006; Dampare et al., 2008, 2009, 2019); Zone 4: Katiola-Marabadiassa and Haute Comoe belts in Ivory Coast (Abouchami et al., 1990; Alric, 1990; Pouclet et al., 1996, 2006); Zone 5: Kadiolo belt in Mali (Sangaré, 2008); and Zone 6: Mako belt in Eastern Senegal (Bassot, 1966; Dia, 1988; Abouchami et al., 1990; Dioh, 1995; Ngom, 1995; Dia et al., 1997; Ngom et al., 1998; Diallo, 2001; Pawlig et al., 2006; Ngom et al., 2007, 2010; Labou, 2019; Labou et al., 2020).

2.2 Kedougou-Kenieba Inlier

The Paleoproterozoic Kedougou-Kenieba Inlier (KKI) located on either side of the Faleme River (Senegal Mali border) is bounded on its western part by the Variscan Mauritanides and unconformably overlain by flat-lying Neoproterozoic sediments of the Taoudeni basin (Bassot, 1966; Bessoles, 1977) (**Fig. 2**). Birimian formations of the KKI are divided into two groups trending NNE-SSW: the western Mako greenstone belt and the eastern Diale-Dalema group (Bassot, 1966).

The western greenstone belt of Mako which has been the subject of numerous studies (see references in Pawlig et al., 2006; Gueye et al., 2007; Theveniaut et al., 2010; Labou et al., 2020) is constituted by the classical sequence of Paleoproterozoic greenstone belts with: i) a tholeiitic series displaying massive and pillowed basalts, gabbro bodies and slices of UM rocks; basalts are interlayered with volcanoclastic sediments, immature detrital sediments and locally limestones (Bassot, 1966; Debat et al, 1984; Ngom, 1985; Diallo, 1994); ii) a differentiated calc-alkaline series comprising bodies and veins of gabbros, basalts, andesites, dacites, rhyolites cross-cutting the tholeiitic rocks and the plutons of granitoids, the amphibole-bearing granitoid of Badon-Kakadian, Tinkoto, Mamakono and Soukouta, the clinopyroxene and orthopyroxene granitoids of Sansankhoto and the biotite-bearing granite of Kenieba (Bassot, 1966; Debat et al., 1984; Dioh et al., 2006; Gueye et al., 2008).

The Diale-Dalema series has been recently subdivided into three entities (Lawrence et al., 2013; Lambert-Smith et al., 2016; Masurel et al., 2017): i) the western Diale-Dalema series consisting of volcanoclastic, siliciclastic and carbonate rocks intruded by the Saraya biotite-bearing batholith (Bassot, 1966); ii) the Faleme Volcanic Belt cropping out to the east of the Diale-Dalema series consisting of volcanic calc-alkaline sequence intruded by the Balangouma and Boboti clinopyroxene granitoids (Ndiaye et al., 1997); iii) the Kofi series consisting of detrital sedimentary and carbonate rocks intruded by the Gamaye pluton. The Faleme volcanic belt and the Kofi series are separated by a NS trending regional sinistral brittle-ductile shear zone: the Senegal-Mali shear zone (SMSZ; Bassot and Dommanget, 1986; Lambert-Smith et al., 2016; Allibone et al., 2020; Diallo et al., 2020).

The boundary between the Mako greenstone belt and the Diale-Dalema series corresponds to a regional shear zone system, 20-30 km wide striking NNE-SSW called the “Main Transcurrent Zone” by Ledru et al. (1989, 1991) and followed by Pawlig et al. (2006), Gueye et al. (2007, 2008), Theveniaut et al. (2010), Lambert-Smith et al. (2016) and Dabo et al. (2017) and conjugate shear-zones, which are oriented NNW-SSE (Theveniaut et al., 2010). During the Eburnean orogeny the KKI has encompassed polycyclic deformation phases (Debat et al., 1984; Bassot et Dommanget, 1986; Ledru et al., 1989; Milesi et al., 1989; Ledru et al., 1991; Pons et al., 1992; Ngom, 1995; Diene et al., 2015; Lambert-Smith et al., 2016; Dabo et al., 2017; Diatta et al., 2017; Masurel et al., 2017; Allibone et al., 2020; Diallo et al., 2020; Kone et al., 2020), widespread low grade metamorphism, except in the surrounding of the granitic plutons where metamorphism reached amphibolite facies conditions (Bassot, 1966; Ngom, 1985; Ndiaye et al., 1997; Gueye et al., 2008; Ganne et al., 2014; Masurel et al., 2017; Kone et al., 2020), and intrusions of granitoid plutons (Bassot, 1966; Dioh et al., 2006; Gueye et al., 2008).

https://doi.org/10.5194/egusphere-2025-814
Preprint. Discussion started: 11 April 2025

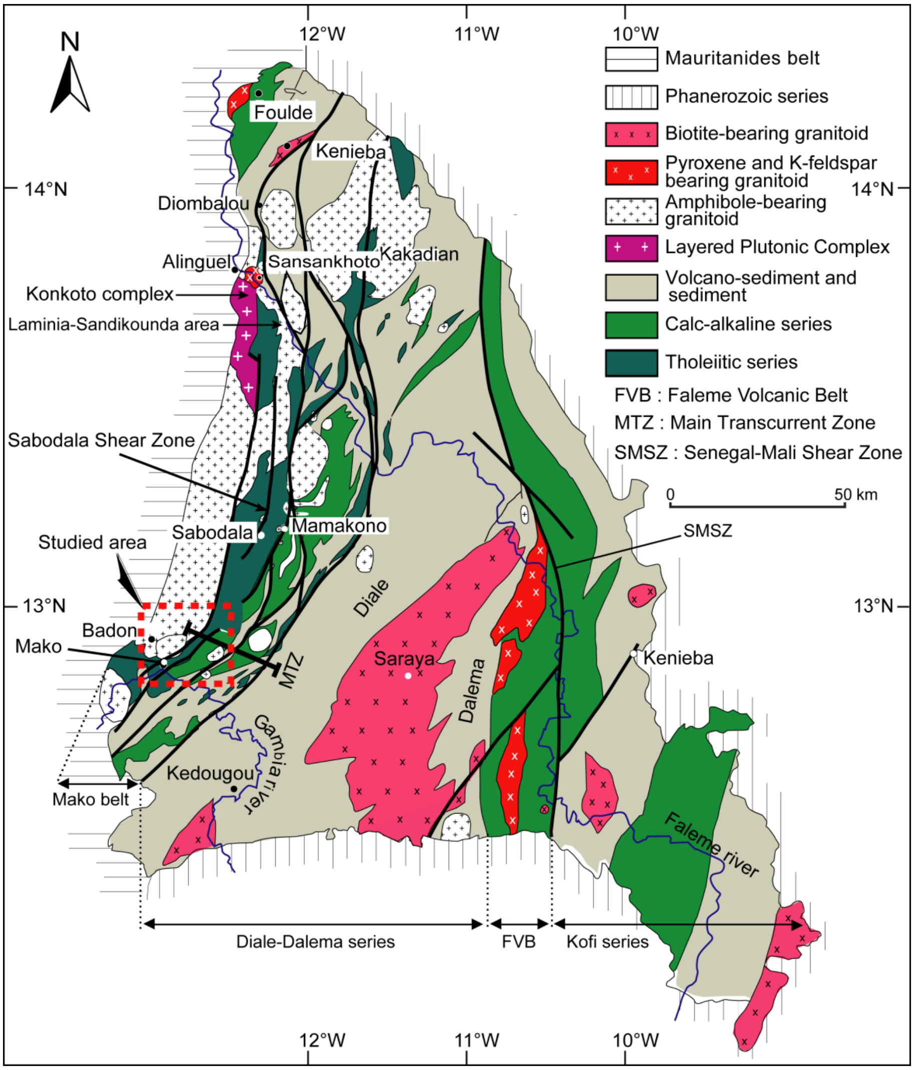

136

137 **Figure 2: Geological map of the Kedougou-Kenieba Inlier (modified from Dioh et al., 2006).**

2.3 The Mako greenstone belt

The characteristics of the Mako greenstone belt have been mainly studied in the SW part of the Mako sector (Fig. 3). This area belonging to the «Main Transcurrent Zone» (MTZ), is the only site where tholeiitic rocks, spatially associated with ultramafic rocks, and calc-alkaline rocks have been recognized. Along the MTZ, the volcanic series are steeply dipping and strongly deformed with development of a schistosity defined by the greenschist facies paragenesis (especially tremolite in the mafic rocks and white micas in the felsic rocks and metasediments). At the boundaries of the slices of UM occurrences, the schistosity becomes mylonitic.

https://doi.org/10.5194/egusphere-2025-814
Preprint. Discussion started: 11 April 2025

The tholeiitic series consists of a thick sequence of locally pillowed basalts interlayered with immature detrital sediments and volcanic sediments, gabbro and UM rocks. Recent studies of the UM rocks based on chemical and isotopic data (Labou et al., 2020) have revealed the existence of two different tholeiitic series, named tholeiitic series 1 consisting of a set of lherzolites and harzburgites and tholeiitic series 2 consisting of wehrlites (**Fig. 3**). The calc-alkaline series is composed by: i) a differentiated sequence of gabbro, basalt, andesite, dacite, rhyolite occurring as dikes cross-cutting the tholeiitic rocks; ii) amphibole-bearing granitoids (southwestern part of the Badon-Kakadian batholith, Tinkoto, Makana, Niemenike, Soukouta rounded plutons). Niemenike and Soukouta plutons are surrounded by a microgranitic aureole (Bassot, 1966; Debat et al., 1984; Dioh et al., 2006).

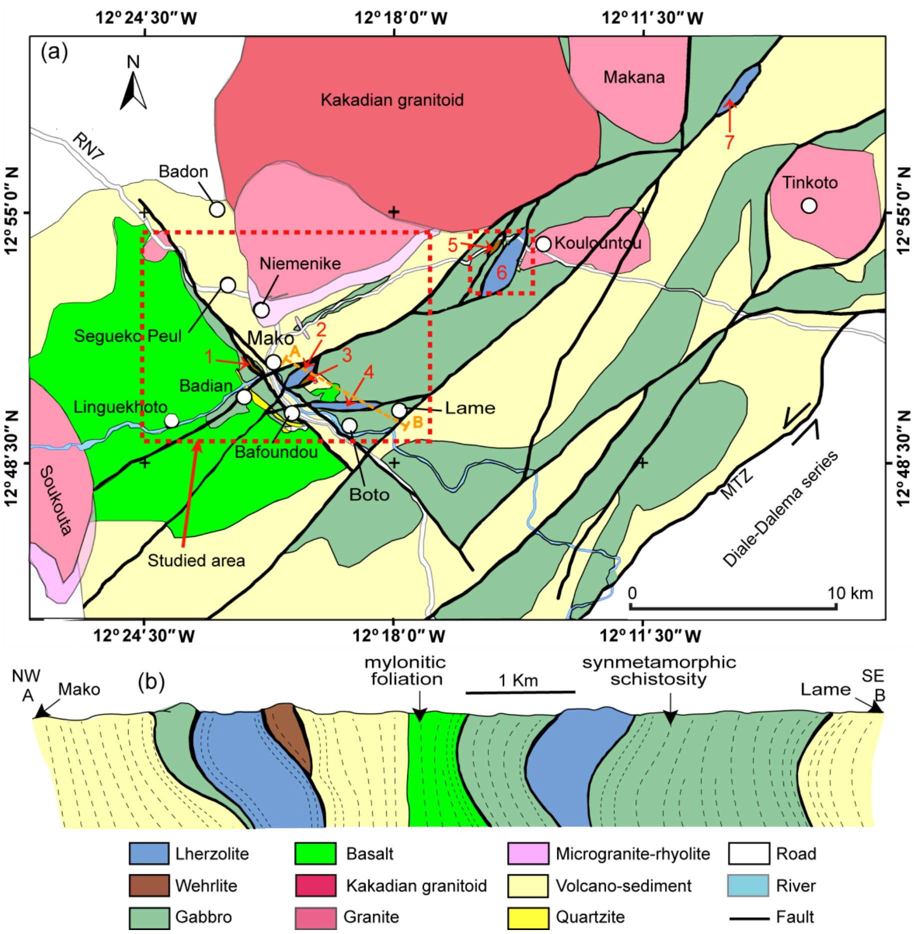

Figure 3: (a) Interpretative geological map of the Mako village area (modified from Theveniaut et al., 2010). 1 represents the western Mako UM massif, 2 and 3 the southeastern Mako UM massifs, 4 the Lame UM massif, 5 and 6 the Kouloutou UM massifs and 7 the Sofia UM massif; (b) Geological section (AB) between the villages of Mako and Lame showing the geometric relationships between the different facies.

https://doi.org/10.5194/egusphere-2025-814
Preprint. Discussion started: 11 April 2025

3 Analytical techniques

45 samples including 11 basalts, 29 gabbros, 4 andesites and 1 dacite hand-specimens were selected in the Mako sector for petrological and geochemical analyses on whole-rock samples. Additionally, minerals such as pyroxene and amphibole were analyzed to determine their major element contents using a Cameca SX Five electron microprobe (Raimond Castaing microcharacterization center in Toulouse; Toulouse III - Paul Sabatier University) with an acceleration voltage of 15 kV, currents of 10 or 20 nA depending on the resistance of the minerals to the electron beam and acquisition times of 10 seconds on the peak and 5 seconds on either side of the peak for the continuous background. The standards used for the measurement of concentration are natural or synthetic minerals as well as pure metals.

The whole-rock samples, were crushed and powdered in an agate mortar, and then the concentrations for major elements were determined by X-ray fluorescence spectrometry (XRF) at the Central Analytical Facilities, Stellenbosch University (South Africa) and ALS (Spain); while trace element analyses, rare earth elements (REE), high field strength elements (HFSE: Th, U, Nb, Y, Zr, Hf) and Cr, Ni, V, Pb, Sn, Sb, W, Mo, Li, Cs, Rb, Ba and Sr were performed at the Geosciences Environnement Toulouse (GET) laboratory (Observatoire Midi-Pyrénées (OMP), University Toulouse III Paul Sabatier (France). Samples were dissolved in acid on a hot plate, in a class 10,000 clean lab following the protocol described by Yokoyama et al. (1999) modified by Rospabé et al. (2018). Trace element concentrations of rocks were obtained by HR-ICP-MS (high Resolution- Inductively Coupled Plasma- Mass Spectrometer) ELEMENT XR (Thermo Scientific TM). Three geostandards (PMS, BCR-2, $BHVO_2$) and two blanks (acid blank 2.5 % HNO_3, chemistry blank) were used to check data reliability, correct the measurements for instrumental drift, and recalculate concentrations.

Rb/Sr and Sm/Nd isotopic measurements were performed at the Geosciences Environnement Toulouse (GET) laboratory in Toulouse, France, using a Finnigan "MAT 261" and Thermo Scientific Triton Plus TIMS at Observatoire Midi Pyrénées, Toulouse. After purification of Sr and Nd in the clean lab according to the protocol written by Pin et al. (1994), these two elements were deposited on rhenium and tungsten filaments respectively using a micro-syringe. Isotopic standards NBS 987 for Sr and La Jolla for Nd gave, during the measurements of this study, 0.710274 ± 40 and 0.511842 ± 20 respectively. Typical procedure blanks are 150 ng for Sr and 24 ng for Nd.

Main petrogeochemical characteristics (Table S1), major and trace concentrations (Table S2), Rb/Sr and Sm/Nd isotopic data (Table S3) of the various rock types from Mako and the main geochemical characteristics of the various types of UM rocks, gabbro and basalt from the WAC (Table S4) are provided in the Supplementary materials.

4 Petrography and geochemistry of minerals and whole rock analyses

An exhaustive sampling of rocks has been carried out from the two major recognized magmatic series, i.e., 1) an ultramafic to mafic tholeiitic series, mainly composed of UM rocks, gabbro, and basalt, and 2) a mafic to differentiated calc-alkaline series, composed of gabbro, basalt, andesite and dacite, which are located in the Mako sector within the MTZ (Ledru et al., 1989, 1991). The rocks of these two series with their sample numbers are located on an outcrop map (**Fig. 4**) and their GPS positions are listed in Table S2. A previous study (Labou et al., 2020) on the ultramafic rocks

https://doi.org/10.5194/egusphere-2025-814
Preprint. Discussion started: 11 April 2025

showed the existence of two tholeiitic series (named as tholeiitic 1 and tholeiitic 2; Table S1). Major and trace concentrations of mafic to differentiated rocks are available in the Table S2.

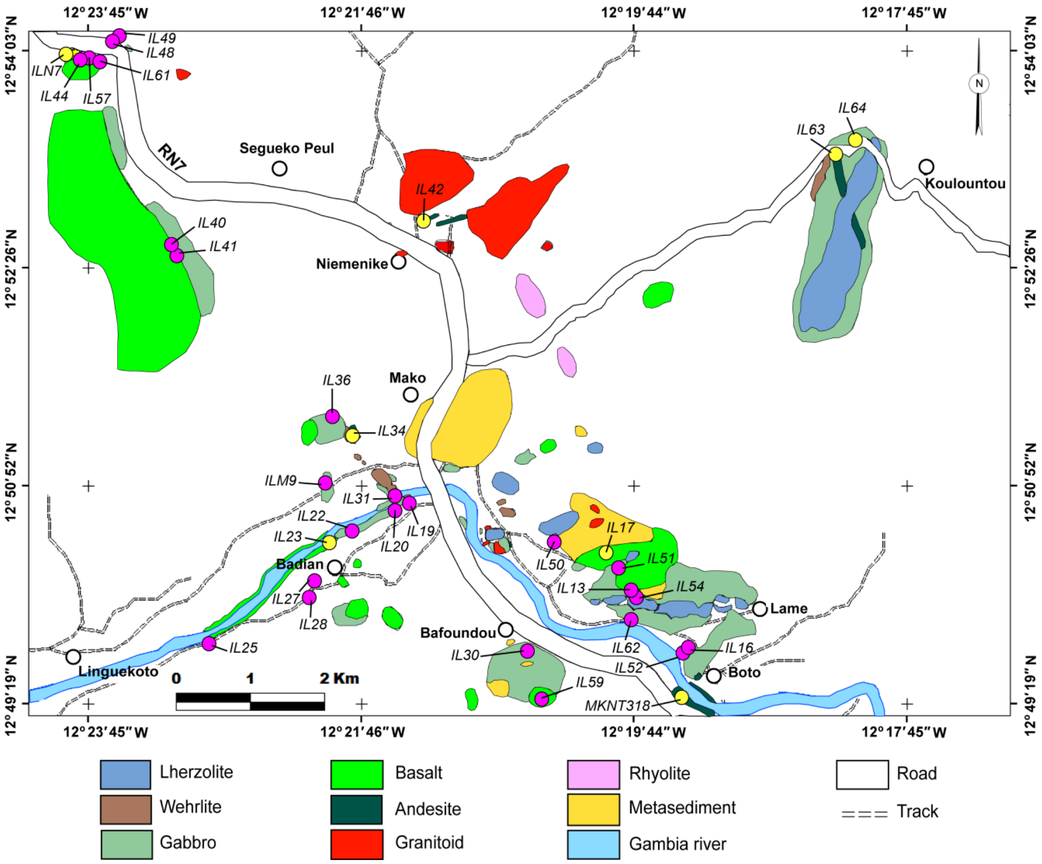

Figure 4: Outcrop map of the Mako area showing the location of the various rock types with sample numbers. The purple circles represent the tholeiitic series and the yellow circles the calc-alkaline series.

4.1 Petrography and geochemistry of the tholeiitic 1 series

Tholeiitic basalts 1 are recognized in the field as pillow lavas (c.f., samples IL4, IL25, IL40, IL48 and IL59; **Fig. 5a**), where pillows can reach up to 1.2 m in size. They show a microlitic and porphyric microlitic textures with a primary paragenesis composed of clinopyroxene (augite Wo_{28-41}, En_{42-58}, Fs_{12-21}; Morimoto et al., 1988) and plagioclase. The secondary paragenesis comprises magnesio-hornblende (Si = 7.4 – 6.6 p.f.u.; X_{Mg} = 0.8 – 0.6; Leake et al., 2003), accompanied by fibers of actinolite and albite. The tholeiitic basalts 1 display contents of SiO_2 varying from 47.8 to 53 wt. %, Al_2O_3 from 11.4 to 15.8 wt. %, Fe_2O_3 from 11.8 to 18.1 wt. %, CaO from 5 to 11.3 wt. % (depending on the modal abundance of the plagioclase), and X_{Mg} values varying from 0.3 to 0.6, depending on the alteration levels of the rock.

https://doi.org/10.5194/egusphere-2025-814
Preprint. Discussion started: 11 April 2025

Tholeiitic gabbros 1 are homogeneous (c.f., samples IL22, IL26, IL27, IL30, IL37, IL41, IL43, IL46, IL47, IL9, IL52, IL53, IL54, IL62, IL66, IL67 and ILM9) and sometimes they are found as small bodies in tectonic contact with the surrounding pillowed basalts (IL41; **Fig. 5b**) or as enclaves in the calc-alkaline basalts (IL53, IL54), dacite (IL5) and granodiorite (IL7). Tholeiitic gabbros 1 show different textures, such as isogranular, porphyroid and pegmatitic, among others. The primary paragenesis consists of plagioclase, clinopyroxene with a composition from augite (Wo_{34-44}, En_{36-54}, Fs_{9-24}) to diopside (Wo_{46-48}, En_{38-41}, Fs_{13-16}), magnesio-hornblende (Si = 7.5 – 7.4 p.f.u.; X_{Mg} = 0.8 – 0.7), chromite, apatite, ilmenite. The well-developed secondary paragenesis comprises fibers of actinolite, albite, epidote, chlorite, titanite, sericite, calcite, quartz and rutile. The tholeiitic gabbros 1 display contents of SiO_2 from 47 to 51 wt. % and Al_2O_3 from 7 to 18 wt. %. X_{Mg} values shows high variations (from 0.4 to 0.7) linked to the evolution of MgO contents from 4.4 to 13.3 wt. %. The high MgO (13 to 16 wt. %) and Cr_2O_3 (from 0.3 to 0.6 wt. %) contents and the relatively low Al_2O_3 (4 to 7 wt. %) and Na_2O (0.1 to 1.3 wt. %) contents of some gabbros (IL66 and 126B) would be related to local accumulation of olivine or chromite; however, fresh olivine has not be recognized in the petrographic characterization.

Plotting silica contents as a function of the immobile elements Zr and Ti (Winchester and Floyd, 1977), these mafic rocks (basalts and gabbros) are classified as basalt and andesite (**Fig. 6a**) of tholeiitic affinity (Th/Nb vs. Zr/Y diagram; Ross and Bédard, 2009). Tholeiitic basalts 1 (ΣREE = 175 – 1,058 ppm) are 9 to 89 times LREE enriched and 10 to 40 times HREE enriched, compared to chondrite composition (**Fig. 7a**). LREE (La_N/Nd_N = 0.9 – 1.1) and MREE (Sm_N/Gd_N = 0.9 – 1.1) patterns are flat and HREE pattern weakly depleted (Dy_N/Lu_N = 1.3 – 1.7). Eu displays negative anomalies (Eu/Eu* where $Eu^* = (Gd \times Sm)^{1/2}$ = 0.7 – 0.9) which are increasingly pronounced in the most REE-rich patterns except for the sample IL59, which is the most REE-poor and the least affected by alteration (presence of unaltered clinopyroxene). On an extended trace elements normalized diagram (**Fig. 7b**), tholeiitic basalts 1 show irregular pattern with a marked negative Zr anomaly, and tholeiitic gabbros 1 (with ΣREE values = 128 – 448 ppm) display moderately enriched in LREE, from 8 to 34 times chondrites and depleted in HREE from 6 to 16 times chondrites. The tholeiitic gabbros 1 also display a marked negative Zr anomaly and positive Pb and Sr anomalies (**Fig. 7b**).

Tholeiitic ultramafic rocks 1 occur as kilometric slices tectonically emplaced within the basalts, gabbros and metasediments (slices 2 and 4 of Lame, slice 6 of Koulountou and slice 7 of Sofia; **Fig. 3**). Their characteristics have been detailed in Labou et al. (2020). They principally consist of lherzolite with minor harzburgite (Table S1). Lherzolites present a heteradcumulate texture (**Fig. 5c**). Cumulate minerals are ~ 3 % chromite and ~ 50 % olivine, whereas intercumulus minerals are 35 – 40 % clinopyroxene, 10 % orthopyroxene, and 2 % amphibole. The lherzolites display SiO_2 contents varying from 38.7 to 44.6 wt. %. They are moderately depleted in REE (ΣREE = 35 – 113 ppm) with convex patterns and negative Eu anomaly (Eu/Eu* = 0.8 – 1) (**Fig. 7a**). The harzburgite sample displays lower contents of REE (ΣREE = 70), with a less convex REE pattern and no Eu anomaly.

As a result, it appears that the different components of the tholeiitic series 1 (lherzolite, harzburgite, gabbro, basalt) show several features indicating that these rocks belong to the same series, particularly, the similarity of their flat REE patterns with continuous enrichment (2 to 89 times the chondrites in LREE) from UM to mafic rocks.

https://doi.org/10.5194/egusphere-2025-814
Preprint. Discussion started: 11 April 2025

4.2 Petrography and geochemistry of the tholeiitic 2 series

Tholeiitic basalts 2 occur as pillows (IL57) similarly to basalts 1, or sometimes massive lavas (IL13) with microlitic and porphyritic microlitic textures. They display a primary paragenesis of albitized plagioclase, magnesio-hornblende (Si = 7.4 – 6.6 p.f.u; X_{Mg} = 0.8 – 0.6) and altered clinopyroxene found as ghosts under actinolite lamellae. Basalts 2 display SiO_2 contents from 47 to 50 wt. %, Al_2O_3 from 12.3 to 15.6 wt. %, and Fe_2O_3 ~ 13 wt. %. X_{Mg} values are ~ 0.5. One sample (IL57) is highly altered with high content in SiO_2 (57.7 wt. %) and low content in MgO (1.7 wt. %).

Tholeiitic gabbros 2 are generally homogeneous in their mineralogic composition (samples IL19, IL20, IL33, IL31, IL36, IL11, IL16, IL50), and they are found sometimes layered (sample IL61 in NW to Segueko Peul village) or as a dyke (IL49) intersecting the tholeiitic basalts 1 (IL48) (**Fig. 5g**). The layered gabbro (IL61) shows an alternation of centimetric layers, amphibole-rich black layers and plagioclase-rich clear layers punctuated by a few spots of dark minerals (**Fig. 5d**). Tholeiitic gabbros 2 generally display isogranular, granophyric, pegmatitic textures but sometimes they show texture in rosette where the prismatic clinopyroxene crystals (2 mm long and 0.4 mm wide) define a « bird's feet » arrangement. Tholeiitic gabbros 2 contain a primary paragenesis with plagioclase (An_{54}), augite (Wo_{34-39}, En_{43-48}, Fs_{15-22}) and secondary magnesio-hornblende (X_{Mg} = 0.7 – 0.6). They display SiO_2 contents varying from 47 to 52 wt. %, Al_2O_3 from 6.1 to 18.4 wt. %, MgO from 6.1 to 18.4 wt. %, Fe_2O_3 from 9.1 to 16 wt. %, and X_{Mg} values from 0.3 to 0.8. The variations in the Al_2O_3 contents and X_{Mg} data are related to the variations of the plagioclase and the clinopyroxene modal composition.

Like the mafic rocks of tholeiitic 1 series, basalts and gabbros from tholeiitic 2 series are classified as basalt and andesite with a tholeiitic affinity (**Figs. 6a, b**). Tholeiitic basalts 2 (ΣREE = 298 – 1294 ppm) display REE patterns indicating a slight and regular LREE enrichment (36 to 134 times chondrites), a slight HREE depletion (9 to 42 times chondrites), and negative Eu anomalies (Eu/Eu* = 0.7 – 0.9) (**Fig. 7c**). On an extended trace element normalized diagram tholeiitic basalts 2 show negative Th, Nb, Pb, Sr, Zr and Ti anomalies (**Fig. 7d**). Tholeiitic gabbros 2 (ΣREE = 139 – 944 ppm) are 14 to 120 times chondrites LREE enriched with very steep spectra (La_N/Yb_N = 2.1 – 3.6). These patterns illustrate a progressive depletion of the whole of REE, LREE (La_N/Nd_N = 1.2 – 1.5), MREE (Sm_N/Gd_N = 1 – 1.2) and HREE (Dy_N/Lu_N = 1.4 – 1.7). Europium anomalies are slight (Eu/Eu* = 0.8 – 0.9) (**Fig. 7c**). On an extended trace element normalized diagram (**Fig. 7d**), tholeiitic gabbros 2 display negative Th, Nb, Zr and Ti anomalies and variable Pb, Sr anomalies. The strong positive Sr anomalies occur in plagioclase-rich gabbros (IL11, IL16, IL20 and IL36) where Al_2O_3 contents are up to 12.4 to 14.2 wt. %, whereas negative Sr anomalies occur in clinopyroxene-rich and plagioclase-poor gabbros (IL31 and IL50) with Al_2O_3 contents ranging between 6.1 and 7 wt. %.

Tholeiitic ultramafic rocks 2 (see details in Labou et al., 2020 and main petrogeochemical characteristics summarized in the Table S1) are classified as wehrlites occurring as two types of massifs: i) monolithic massifs cropping out to the west of the villages of Mako (slice 1; samples IL18, IL32) and Koulountou (slice 5; sample 116); and ii) elliptical bodies in tectonic contact with the lherzolites cropping out at Lame (slice 3; samples ILL3, 77) (**Fig. 3**). Wehrlites present a heteradcumulate texture with 3 – 4.5 % chromite, 64 – 73 % olivine, 22 – 26 % clinopyroxene, 3% amphibole and phlogopite (1 %) (**Fig. 5e**). They display a variation of SiO_2 between 38.3 and 41.5 wt. % and high X_{Mg} values (0.8) with MgO contents up to 35 wt. %. Wehrlites have enriched REE and trace element contents (∑REE = 45 – 119 ppm). They are homogeneously fractionated (La_N/Yb_N = 2 – 2.5, **Fig. 7c**) and characterized by weak negative Eu anomalies (Eu/Eu*

https://doi.org/10.5194/egusphere-2025-814
Preprint. Discussion started: 11 April 2025

= 0.9). In an extended normalized trace element diagram (**Fig. 7d**), wehrlites show Nb, Sr and in lesser extent negative Ti anomalies.

As a result, the components of the tholeiitic series 2 (wehrlite, gabbro, basalt) show several characteristics, i.e., parallelism of the slight enriched-LREE patterns with a continuous LREE enrichment from the wehrlites to the gabbros and basalts, (4 to 134 times the chondrites in LREE, **Fig. 7c**), and the same slight negative Th, Nb, Zr and Ti anomalies, indicating that these rocks belong to the same specific magmatic series.

4.3 Petrography and geochemistry of the calc-alkaline series

Calc-alkaline rocks (except for granitoids) occur mainly in the Diale-Dalema basin (Bassot, 1987; Ndiaye et al., 1997; Lawrence et al., 2013a, b; Lambert-Smith et al., 2016), and also crop out in the Mako area (Dia, 1988; Diallo, 1994; Dioh, 1995; Ngom, 1995; Moussolo, 2000; Pawlig et al., 2006; Dioh et al., 2009; Cissokho, 2010; Gozo et al., 2015; Gozo, 2017; Labou, 2019). They correspond to small bodies and veins of a differentiated series: gabbro, basalt, andesite, dacite, and rhyolite that crosscut the tholeiitic formations (**Fig. 6a**). These rocks display a transitional to calc-alkaline signature (Zr/Y vs. Th/Yb diagram; **Fig. 6b**).

Gabbros have a granoblastic texture (IL64 and IL68), more rarely pegmatitic (IL69 and IL125), and are composed of plagioclase and clinopyroxene (augite, Wo_{34-45}, En_{29-50}, Fs_{8-29}), and minor occurrences of amphibole and Fe-Ti oxides. They have SiO_2, TiO_2 and Al_2O_3 values ranging from 51.7 to 55.9 wt. %, 0.8 to 0.9 % wt. % and 14.8 to 15.1 wt. %, respectively. They are REE enriched (ΣREE = 326 – 399 ppm), with concentrations from 51 to 69 times chondrites for LREE (La_N/Sm_N = 2.4 – 2.7) and highly depleted from 7 to 1 times chondrites for HREE (Gd_N/Yb_N = 1.7 – 1.9). This results in a strongly negative slope of the REE patterns (La_N/Yb_N = 5.5 – 5.7) (**Fig. 7e**). Eu anomaly is weakly negative (Eu/Eu* = 0.8 – 0.9). In an extended normalized trace element diagram (**Fig. 7f**), gabbros show negative Nb and Ti anomalies.

Basalts have the same mineralogy as gabbros but are microlitic in texture (IL23). They nearly display the same major elements composition except for SiO_2 contents which reach 54.9 to 55.8 wt. %. These high SiO_2 contents are linked to the occurrences of amygdale textures filled with quartz and albite (IL17). The basalts REE patterns are steeply sloping (La_N/Yb_N = 5.7 – 8.2) with a LREE enrichment (La_N/Sm_N = 2.4 – 2.9) from 70 to 109 times chondrites and a clear depletion in HREE (Gd_N/Yb_N = 1.8 – 2.1) from 10 to 11 times chondrites. They display weak negative Eu anomalies (Eu/Eu* = 0.8 – 0.9) and strong negative Nb, Sr and Ti anomalies (**Figs. 7e, f**).

Andesites display two types of texture and mineralogical composition: i) andesite showing a microlitic porphyry texture with either plagioclase (IL34; **Fig. 5f**) or clinopyroxene phenocrysts (augite Wo_{33-41}, En_{42-53}, Fs_{10-21}) (ILN7); ii) andesite with a microlitic texture (IL42) rich in magmatic amphibole (pargasite, tschermakite and magnesio-hornblende (X_{Mg} = 0.9 – 0.6). Andesites show SiO_2 values ranging from 49.7 to 58.2 wt. %, high CaO and Na_2O contents ranging from 8.8 to 10.1 wt. % and 2.8 to 7.6 wt. %, respectively. These values are linked to secondary alterations: carbonatation (samples IL42 and ILN7) and albitisation (sample IL 34). Andesites with ΣREE = 544 – 703 ppm are LREE enriched (La_N/Sm_N = 2.2 – 3.1) from 91 to 124 times chondrites and HREE depleted (Gd_N/Yb_N = 1.6 – 3) from 8 to 22 times chondrites. Eu

https://doi.org/10.5194/egusphere-2025-814
Preprint. Discussion started: 11 April 2025

anomalies are weakly negative (Eu/Eu* = 0.7 – 0.8) (**Fig. 7e**). On an extended trace element normalized diagrams, andesites show negative Th, Nb, Pb, Sr and Ti anomalies (**Fig. 7f**).

Dacite sample (IL5) shows a porphyritic texture and is mainly composed of the Mg-hornblende type phenocrysts (Si = 6.9 – 6.8 a.p.f.u.; XMg = 0.7 – 0.6) and plagioclase phenocrysts exhibiting oscillatory zoning in a matrix of microlites of amphibole, plagioclase, biotite, and quartz. The dacite with relatively low SiO_2 (62 wt. %) and Al_2O_3 (15 wt. %) contents is, compared to the chondrites, 101 times enriched in LREE (La_N/Sm_N = 3.5), and 6 times depleted in HREE (Gd_N/Yb_N = 2.5). This results in a highly tilted pattern (La_N/Yb_N = 14) with a weak negative Eu anomaly (Eu/Eu* = 0.8) (**Fig. 7e**). In the extended pattern, the dacite shows enrichment in LILE, negative anomalies in Th, Nb, Ti and positive anomalies in Pb and Sr (**Fig. 7f**). In summary, the rocks of the calc-alkaline series show common features of a high aluminous character, such as depletion in Cr_2O_3, REE fractionation and negative Nb and Ti anomalies, suggesting that they belong to the same specific magmatic series.

https://doi.org/10.5194/egusphere-2025-814
Preprint. Discussion started: 11 April 2025

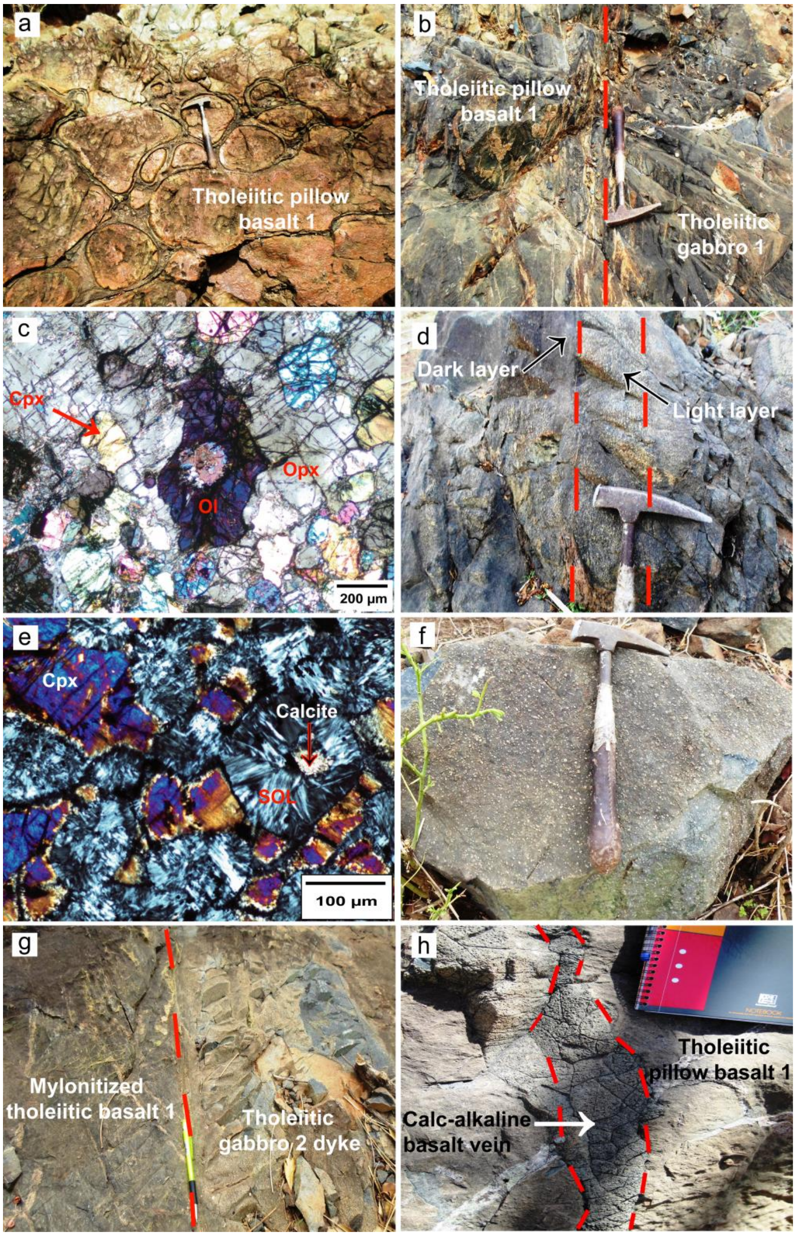

Figure 5: (a) Badian tholeiitic basalt 1 (IL25) showing pillow lavas; (b) tectonic contact between tholeiitic pillow basalt 1 (IL40) and tholeiitic gabbro 1 (IL41) in the Niemenike quarry; (c) photomicrograph in XPL of the granular lherzolite 1 of Kouloutou (IL9) showing poikilitic orthopyroxene (Opx) hosting small crystals of olivine (Ol) and clinopyroxene (Cpx); (d) tholeiitic gabbro 2 layer of Segueko Peul (IL61) showing alternating light and dark layers; (e) photomicrograph in XPL of the wehrlite 2 of west Mako (IL32) showing intercumulus clinopyroxene (Cpx) and cumulus olivine completely altered in serpentine (SOL),

https://doi.org/10.5194/egusphere-2025-814
Preprint. Discussion started: 11 April 2025

calcite and Fe-oxides; (f) porphyritic calc-alkaline andesite of west of Mako village showing phenocrystals of plagioclase (IL34); (g) a REE-enriched tholeiitic gabbro 2 dyke (IL49) intersecting a mylonitized REE-flat tholeiitic basalt 1 (IL48) in Segueko Peul; (h) Vein of calc-alkaline basalt (IL23) cross-cutting pillowed tholeiitic basalt 1, Lame area.

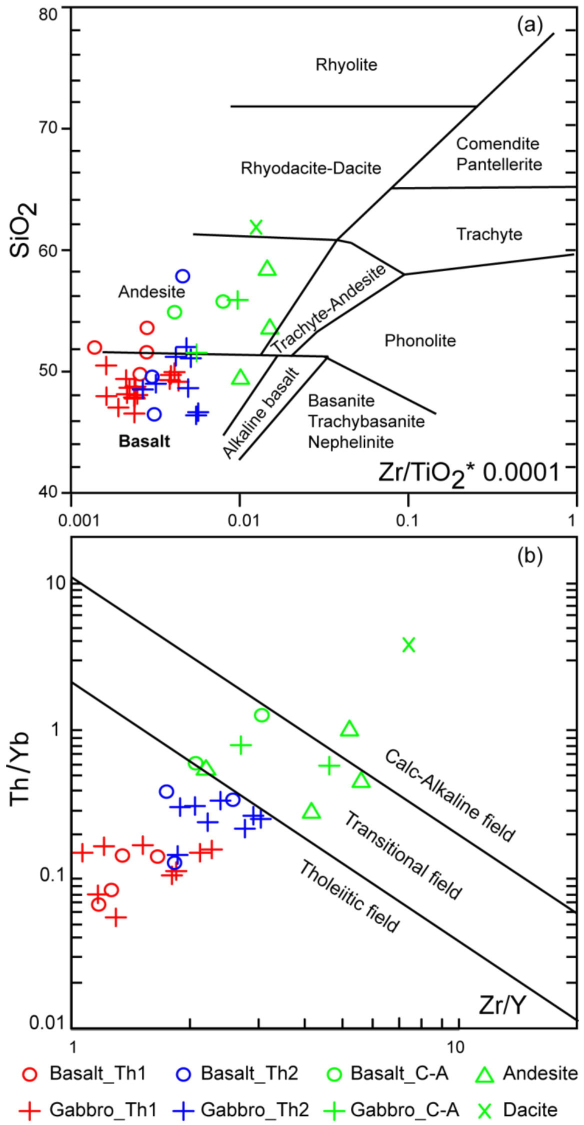

Figure 6: Discrimination plots for the magmatic rocks of the Mako greenstone belt. (a) diagram of SiO_2 vs. $(Zr/TiO_2)\times0.0001$ of Winchester and Floyd (1977); (b) diagram of Th/Nb vs. Zr/Y of Ross and Bédard (2009). Abbreviations: Th1 = Tholeiitic 1 series, Th2 = tholeiitic 2 series; C-A = Calc-alkaline.

https://doi.org/10.5194/egusphere-2025-814
Preprint. Discussion started: 11 April 2025

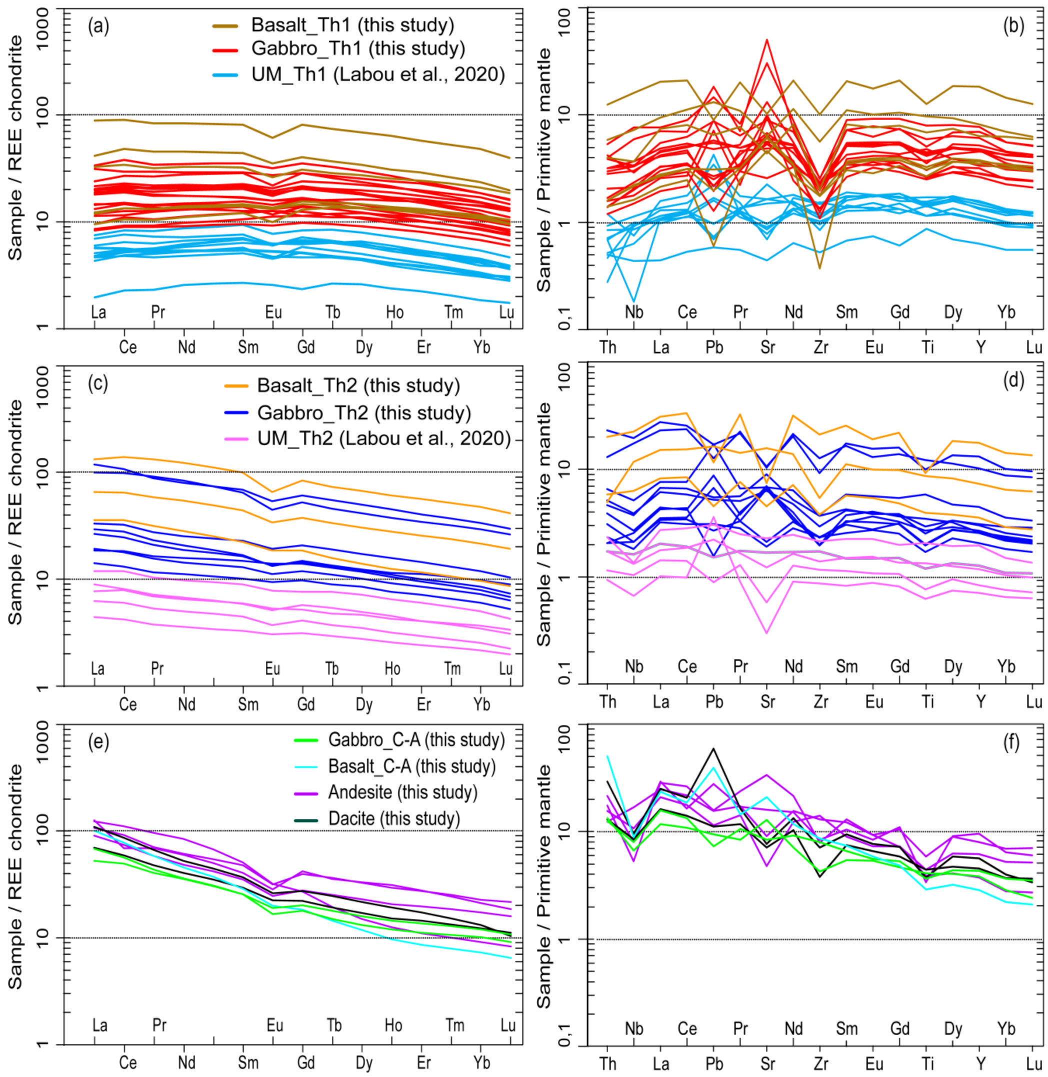

Figure 7: REE diagram normalized to NWA974 chondrites (Barrat et al., 2014) and multi-elements diagram normalized to the Primitive Mantle (Sun and McDonough, 1989) for tholeiitic series 1 (a and b), tholeiitic series 2 (c and d) and calc-alkaline series (e and f). For symbol abbreviations, see Fig. 6.

4.4 Nd and Sr isotopic signatures

Sr and Nd isotopic measurements were performed on 28 samples from tholeiitic 1 series, 13 from tholeiitic 2 series and 8 from calc-alkaline series (Table S3). In addition, 14 ultramafic rock samples have already been studied in detail in Labou et al. (2020).

It is worth noting that the Rb/Sr and Sm/Nd data, reported in isochron diagram, are aligned along an isochron calculated at about 2.1 Ga (**Fig. 8**). The data presents some heterogeneities for the Rb/Sr and Sm/Nd systems, which may be due to the greenschist metamorphism. Nevertheless, in absence of reliable geochronological dating on these rocks, the initial $^{87}Sr/^{86}Sr$, $^{143}Nd/^{144}Nd$, and εNd ratios were calculated for an age of 2.1 Ga considered to be the age of formation or accretion of the Paleoproterozoic crust during the Eburnean orogeny (Abouchami et al., 1990; Boher et al., 1992; Dia et al., 1997; Pawlig et al., 2006; Ngom et al., 2010; Labou et al., 2020). The tholeiitic series 1 samples (n = 19) are characterized by initial $^{87}Sr/^{86}Sr$ (2.1 Ga) from 0.70083 to 0.70368, and $^{143}Nd/^{144}Nd$ (2.1 Ga) from 0.50987 to 0.51019, with εNd (2.1 Ga) between -1 to +5.3. The tholeiitic series 2 samples (n = 10) have initial $^{87}Sr/^{86}Sr$ (2.1 Ga) between 0.70139 and 0.70299, and $^{143}Nd/^{144}Nd$ (2.1 Ga) varying between 0.51002 and 0.51027, with εNd (2.1 Ga) values from +1.8 and +6.9. Finally, the calc-alkaline series samples (n = 10) have initial $^{87}Sr/^{86}Sr$ (2.1 Ga) ratios ranging from 0.69615 (certainly overcorrected) to 0.70655, those of $^{143}Nd/^{144}Nd$ (2.1 Ga) ranging from 0.51002 to 0.51015, with εNd (2.1 Ga) values ranging from +2.1 to +4.5.

As a main result, it is not possible to distinguish the three series in terms of isotopic compositions, both for Sr and Nd. The error propagation of the age correction, due to the uncertainty and variability of the father/daughter ratios, avoid any clear distinction between the source of those series. Unlike previous work in the Mako belt (Ngom, 1995; Pawlig et al., 2006) and unlike several provinces in the WAC where contamination by an Archaean component has been suggested (Boher et al., 1992 in Guinea; Kouamélan et al., 1997a, 2018 in Ivory Coast and Dampare et al., 2019 in Ghana), the positive εNd values (2.1 Ga) measured in our samples support the absence or the negligible effect of continental crust contamination.

As far as initial Sr isotopic compositions are concerned, although they are above the depleted mantle of 2 Ga ago, they appear to be very poorly radiogenic. Such signatures have been described in papers by Boher et al. (1992) and Abouchami et al. (1990), but little discussed. Indeed, the Rb/Sr system is more sensitive to the effects of alteration and metamorphism, and therefore more easily disturbed. The statistical consistency of our results, however, indicates that a slightly contaminated depleted mantle type source should be taken into consideration.

https://doi.org/10.5194/egusphere-2025-814
Preprint. Discussion started: 11 April 2025

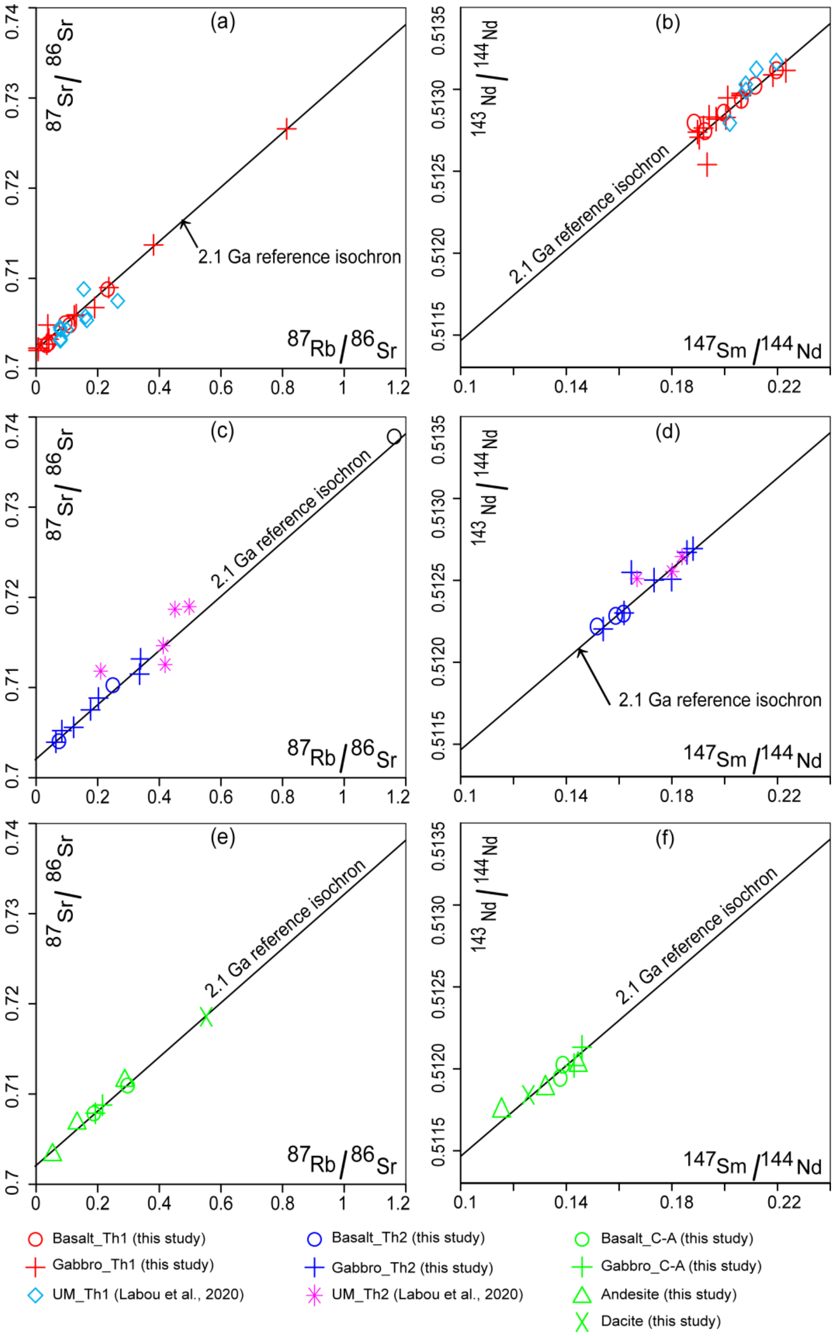

Figure 8: Rb/Sr and Sm/Nd isochron diagrams in which a hypothetical 2.1 Ga calculated isochron is reported of rocks of the three magmatic series of the Mako greenstone belt. For symbol abbreviations, see Fig. 6.

4.5 Relative timing of emplacement of the magmatic series

Two tholeiitic and one calc-alkaline series have been identified in the Mako greenstone belt, mainly based on their trace element compositions. The two tholeiitic series can be discriminated by the La_N/Yb_N vs La_N/Sm_N ratios (**Fig. 9a**), and this result is consistent with the outcrop descriptions, in which we have recognized the two series geometrically separated; in Segueko Peul sector we have identified a dyke of REE-enriched tholeiitic gabbro (IL49) crosscutting a REE-flat tholeiitic basalt layer (IL48) (**Fig. 5g**). Geochemical and field evidence allows us to establish a relative chronological order, with a tholeiitic series 1 composed of basalt-andesites, gabbros and lherzolites (harzburgites), which is characterized by a flat REE pattern, and a tholeiitic series 2 composed of basalt-andesites, gabbros and wehrlites, characterized by a slightly REE enriched pattern. The calc-alkaline series, mainly composed of gabbro-basalt to felsic volcanic rocks, would be the last to set in place as it occurs as veins or bodies intersecting the tholeiitic series (**Fig. 5h**). It is the most enriched series with the most marked negative Nb and Ti anomalies and differs from the two tholeiitic series by its highest La_N/Yb_N and La_N/Sm_N ratios.

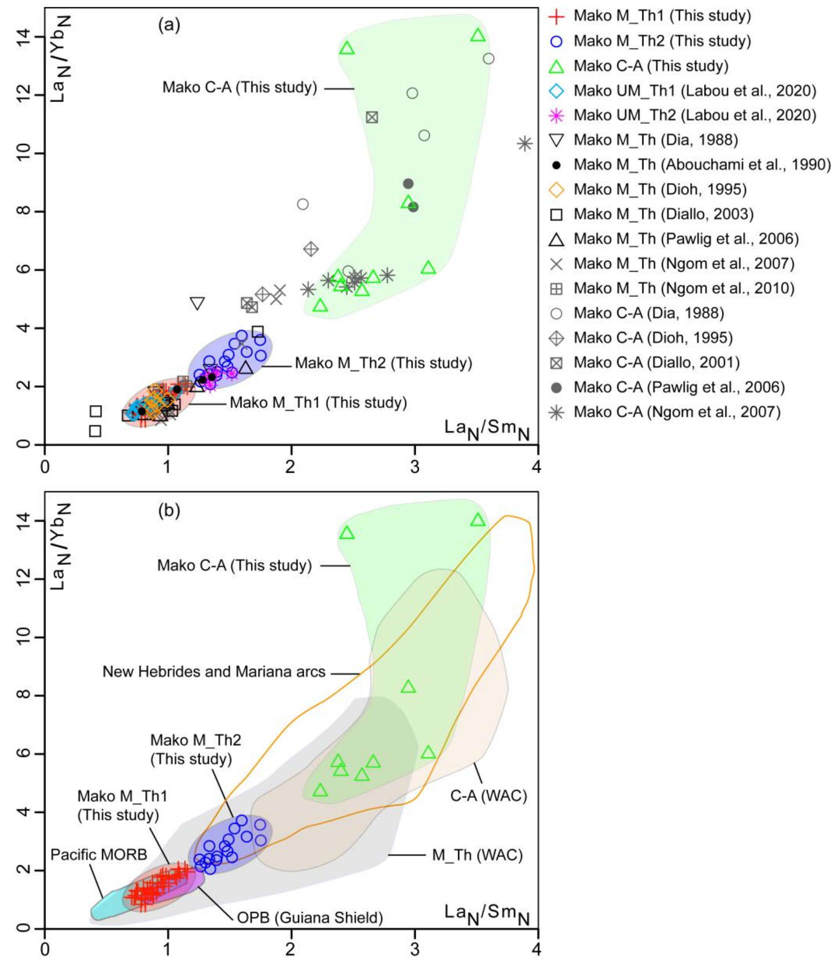

https://doi.org/10.5194/egusphere-2025-814
Preprint. Discussion started: 11 April 2025

Figure 9: La_N/Yb_N vs La_N/Sm_N diagram to discriminate the different magmatic series. (a) comparison with magmatic rocks from Mako greenstone belt (Dia, 1988; Abouchami et al., 1990; Dioh, 1995; Diallo, 2001; Pawlig et al., 2006; Ngom et al., 2007, 2010; Labou et al., 2020) and (b) comparison with magmatic rocks from WAC (Zonou, 1987; Vidal and Alric, 1994; Ama Salah et al., 1996; Pouclet et al., 1996; Loh et al., 1999; Béziat et al., 2000; Attoh et al., 2006; Sangaré, 2008; Dampare et al., 2008, 2009; Baratoux et al., 2011; Senyah et al., 2015; Augustin and Gaboury, 2017; Sakyi et al., 2017; Dampare et al., 2019; Mériaud et al., 2020; Agra et al., 2023; Hayman et al., 2023) and from different current geotectonic sites [Pacific MORB (Bach et al., 1995; Castillo, 2000); OPB Paleoproterozoic, Guiana Shield, Venezuela, 120 Ga (Velasquez et al., 2011); New Hebrides arc tholeiitic (Peate et al., 1997) and Mariana arc calc-alkaline (Bloomer et al., 1987, 1989; Lin et al., 1989; Elliott et al., 1997)]. Abbreviations: M = Mafic; UM = Ultramafic; Th = Tholeiitic; C-A = Calc-alkaline.

5 Discussion

5.1 Comparison with previous work in the Mako belt and throughout the entire WAC

The two tholeiitic series here characterized can be compared with previously studied mafic series in the Mako greenstone belt and other greenstone belts of the WAC, by plotting a La_N/Yb_N vs La_N/Sm_N diagram (**Fig. 9b**). Results from previous works can be summarized (Table S4) as follows: in some areas of the Mako greenstone belt, only one type of tholeiites has been recognized. For example, in the north of the Kedougou Kenieba Inlier (Konkoto complex; **Fig. 2**), gabbros and basalt show low La_N/Yb_N and La_N/Sm_N ratios like the tholeiitic 1 series (Dioh, 1995) while in the Laminia-Sandikounda area (**Fig. 2**), basalt shows slightly higher ratios like those of the tholeiitic 2 series (Dia, 1988). In the central (Sabodala area) and southern (Mako area) parts of the Mako belt, the tholeiitic series has been described as heterogeneous showing depleted and fractionated REE spectra without distinguishing two separated suites (Abouchami et al., 1990; Ngom, 1995; Diallo, 2001; Pawlig et al., 2006; Ngom et al., 2007, 2010). The komatiitic basalts recognized by Ngom (1995) in the Sabodala area show La_N/Yb_N and La_N/Sm_N ratios like those of tholeiitic series 2. The UM series, only being recognized in the Mako area, have also been considered as homogeneous and belonging to a single entity (Ngom, 1995; Ngom et al., 1998; 2010; Cissokho, 2010; Dabo et al., 2017). However, Labou et al. (2020), using the geochemical data of the rocks and clinopyroxenes, defined two tholeiitic UM complexes: i) the first one constituted by a lherzolite + harzburgite assemblage linked to the tholeiitic series 1; and ii) the second one represented by wehrlite linked to the tholeiitic series 2.

Throughout the WAC, several authors have recognized two mafic tholeiitic series characterized by contrasted REE patterns: Ama Salah et al. (1996) in the Liptako area (Niger), Pouclet et al. (1996) in the Haute Comoe area (Ivory Coast), Dampare et al. (2008, 2009) in the Ashanti belt (Ghana), and Baratoux et al. (2011) in the Boromo and Hounde belts (Burkina Faso). On the other hand, only one type of tholeiite, like our tholeiites 1 has been observed in the Haute Comoe area in Ivory Coast by Vidal and Alric (1994) and Hayman et al. (2023), in Ghana by Loh et al. (1999) and Agra et al. (2023), in the Kadiolo belt in Mali by Sangaré (2008), in the Yaoure belt in Ivory Coast by Mériaud et al. (2020), and in Mana gold district in Burkina Faso by Augustin and Gaboury (2017). In the WAC, tholeiitic UM rocks were considered as belonging to a single magmatic entity, with examples in Ashanti (Ghana; Loh et al., 1999; Attoh et al., 2006; Dampare et al., 2019), Katiola-Marabadiassa (Ivory Coast; Pouclet et al., 2006), Bouroum Yalogo (Burkina Faso; Ouédraogo, 1985), and in Kadiolo (Mali; Sangaré, 2008); while in the Mako greenstone belt, Labou et al. (2020) distinguished two types of UM belonging to the two series. Finally, the compositional diversity of the Mako calc-alkaline series overlaps

https://doi.org/10.5194/egusphere-2025-814
Preprint. Discussion started: 11 April 2025

that of all the calc-alkaline rocks in the KKI (Diallo, 2001; Ngom et al., 2007) and the entire WAC (Ama Salah et al., 1996 at Liptako, Niger; Béziat et al., 2000 at Loraboue, Burkina Faso; Dampare et al., 2008 at Ashanti, Ghana, Sangaré, 2008 at Kadiolo, Mali, and Senyah et al., 2015 and Sakyi et al., 2017, Ghana).

The isotopic data was also used to compare with previous work carried out in Mako greenstone belt and throughout the WAC. All data are reported in a $\varepsilon Nd_{(2.1\ Ga)}$ vs α(Sm/Nd) factor (DePaolo and Wasserburg, 1976; DePaolo, 1988) (**Fig. 10**). This diagram shows that the samples of Mako greenstone belt, as well as all samples of Paleoproterozoic age from the WAC (Abouchami et al., 1990; Alric, 1990; Boher et al., 1992; Ama Salah et al., 1996; Dia et al., 1997; Gasquet et al., 2003; Pawlig et al., 2006; Dampare et al., 2009; Ngom et al., 2010; Dampare et al., 2019; Labou et al., 2020), plot along a line named as the "Paleoproterozoic mantle correlation line" (**Fig. 10**), which can be distinguished from the present-day mantle correlation line (defined, for example, by the East Pacific Rise (EPR), the Mariana and New Hebrides arcs). The difference between the two mantle correlation lines is related to the isotopic evolution of the upper mantle, which was less radiogenic during the Paleoproterozoic. Lastly, **Figure 10** shows chemical composition from various magmatic rocks in the entire WAC and the Guiana Shield Craton and highlights the differences of the three magmatic series identified in the Mako greenstone belt.

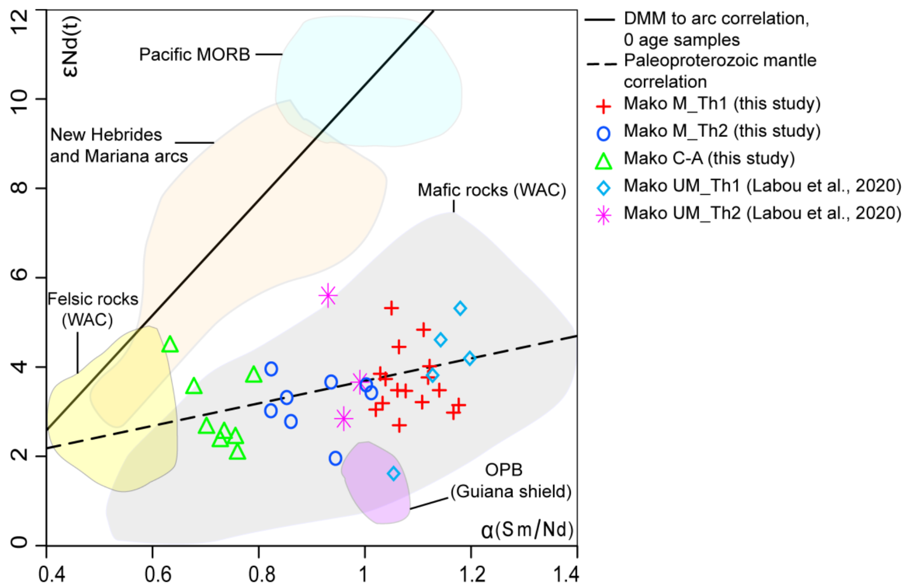

Figure 10: Diagram εNd (t) vs α(Sm/Nd) showing the position at different locations of the three magmatic series on the Paleoproterozoic mantle correlation line (Abouchami et al., 1990; Alric, 1990; Boher et al., 1992; Ama Salah et al., 1996; Gasquet et al., 2003; Pawlig et al., 2006; Dampare et al., 2009; Ngom et al., 2010; Dampare et al., 2019; Labou et al., 2020) off the current mantle correlation line on which align the rocks of the Pacific MORB (Cohen et al., 1980; Hofmann et al., 1983; Byers et al., 1986; Macdougall et al., 1986; Hekinian et al., 1989; Natland, 1989; Prinzhofer et al., 1989; Ben othman et al., 1990; Mahoney et al., 1993; Bach et al., 1995; Batiza et al., 1996; Nui et al., 1999; Regelous et al., 1999; Castillo et al., 2000), New Hebrides arc (Peate et al., 1997) and Mariana arc (Meijer, 1976; Meijer et al., 1981; Hickey et al., 1982; Stern et al., 1984;

https://doi.org/10.5194/egusphere-2025-814
Preprint. Discussion started: 11 April 2025

White et al., 1984; Hawkins et al., 1985; Bloomer et al., 1987; Volpe et al., 1987; Woodhead, 1988; Bloomer et al., 1989; Lin et al., 1989; Hawkins et al., 1990; Stern et al., 1990; Volpe et al., 1990; Hickey-Vargas, 1991; Stern et al., 1991; Alt et al., 1993; Stolper et al., 1994; Gribble et al., 1996; Elliott et al., 1997; Pickett et al., 1997; Gribble et al., 1998; Hickey-Vargas, 1998; Ikeda et al., 1998; Newman et al., 2000). The composition of the Paleoproterozoic OPBs from the Guiana Shield, Venezuela (Velasquez et al., 2011) has also been reported.

5.2 Tectonic setting and magmatic source

Three magmatic series have been discriminated in the Mako greenstone belt based on their REE (**Figs. 7** and **9**) and isotopic signatures (**Figs. 8** and **10**). For the WAC greenstone belts, the tectonic setting is still a subject of research, and several models have been proposed, including mid-ocean ridge, oceanic plateaux, or intra-oceanic arc setting (e.g., Grenholm et al., 2019 for an overview). To develop petrogenetic interpretations for Precambrian rocks, immobile elements, such as HFSE and REE, are preferentially considered in the discrimination diagrams (Condie, 2003, 2005). Indeed, Condie (2005) indicated that ratios using the HFSE and REE are the most relevant relationships for discussing tectonic setting and mantle source composition, because these elements have similar incompatibilities in the mantle. In the La_N/Sm_N vs La_N/Yb_N diagram (**Fig. 9b**), tholeiites from series 1 plot in the same field as the mid-ocean ridge basalt (MORB) and oceanic plateau basalt (OPB), including both Paleoproterozoic series, e.g., Guiana Shield (Velásquez et al., 2011); Burkina Faso (Zonou, 1987); Mako greenstone belt (Ngom et al., 2007; Pawlig et al., 2006); Ghana (Agra et al., 2023) as well as Phanerozoic examples, e.g., Pacific oceanic rocks (Bach et al., 1995; Castillo, 2000). Regarding tholeiites from series 2, they plot in a transitional field between OPB and arc related basalt (ARC) domains, which is a similar behaviour to other Paleoproterozoic belts, e.g., Liptako in Niger (Ama Salah et al., 1996); Mako greenstone belt (Pawlig et al., 2006); Boromo and Hounde in Burkina Faso (Baratoux et al., 2011) as well as the Phanerozoic examples, e.g., New Hebrides in the Pacific Ocean (Peate et al., 1997). Finally, the calc-alkaline series are plotted in the same field as other island-arc basalt (IAB), regardless of their age, e.g., in the WAC, Liptako in Niger (Ama Salah et al., 1996), Mako greenstone belt (Diallo, 2001; Pawlig et al., 2006; Ngom et al., 2007), Loraboue in Burkina Faso (Béziat et al., 2000) as well as Mariana Arc (Bloomer et al., 1987, 1989; Lin et al., 1989; Elliott et al., 1997) and the New Hebrides Arc (Peate et al., 1997).

Regarding the tectonic setting discrimination, Tomlinson and Condie (2001) proposed that a negative Nb anomaly is the most significant difference between the arc and oceanic plateau and/or mid-ocean ridge setting, being it only displayed by the arc volcanic rocks. In our case, the calc-alkaline series show this clear anomaly, implying an arc setting for the formation of these rocks. On the other hand, while tholeiitic rocks of the series 1 show no Nb anomaly, those from series 2 display a slight negative Nb anomaly. This implies that rocks of series 1 would have been emplaced in an OPB setting or in a divergent domain like a MORB setting, whereas those of series 2 could be emplaced in a transitional environment between MORB-OPB and an island arc setting. The Zr/Nb vs. Nb/Th, and Nb/Y vs. Zr/Y diagrams (**Figs. 11a, b**) proposed by Condie (2005), are commonly used to distinguish between MORB and OPB tectonic settings in Paleoproterozoic greenstone belts studies, such as Velásquez et al. (2011) in the Guiana Shield, as well as Agra et al. (2023) in the WAC. **Figure 11** shows that tholeiitic series of Mako greenstone belt do not plot in the MORB field, but in the OPB and OIB domains (**Fig. 11a**). Additionally, both tholeiitic series are plotted above the ΔNb line (**Fig. 11b**), indicating that their

https://doi.org/10.5194/egusphere-2025-814
Preprint. Discussion started: 11 April 2025

source can be associated with a mantle plume, and they were emplaced in an oceanic plateau setting. On the other hand, the calc-alkaline series are plotted on both sides of the ΔNb line (**Fig. 11b**).

To discuss the mantle source, **Figure 10** shows a strong correlation between εNd (2.1 Ga) and α(Sm/Nd) values of the present-day mantle correlation line, reflecting the higher or lower fertility of the upper mantle. This enrichment may be either inherited from the deep mantle (hot-spot like) of from a subduction input (arc-related mantle wedge) A similar correlation is found in both average εNd and α(Sm/Nd) values for the whole WAC magmatic rocks, and this correlation suggests that: (i) the tholeiites from series 1 are characterized by a slightly juvenile signature extracted from a depleted mantle (α(Sm/Nd) between 1.02 and 1.2 and positive εNd), similar to the values presented by the OPBs from the Guiana Shield, Venezuela (Velásquez et al., 2011); ii) tholeiites from series 2 have lower α(Sm/Nd) (0.82 – 1.01) and variable εNd values, suggesting that these rocks could have originated from an enriched mantle component, which is characteristic for volcanic rocks emplaced in a transitional setting between OPB and ARC tectonic settings; iii) calc-alkaline series have the lowest α(Sm/Nd) and more heterogeneous εNd values, indicating obviously that they can be derived from a more enriched source and formed in an island arc.

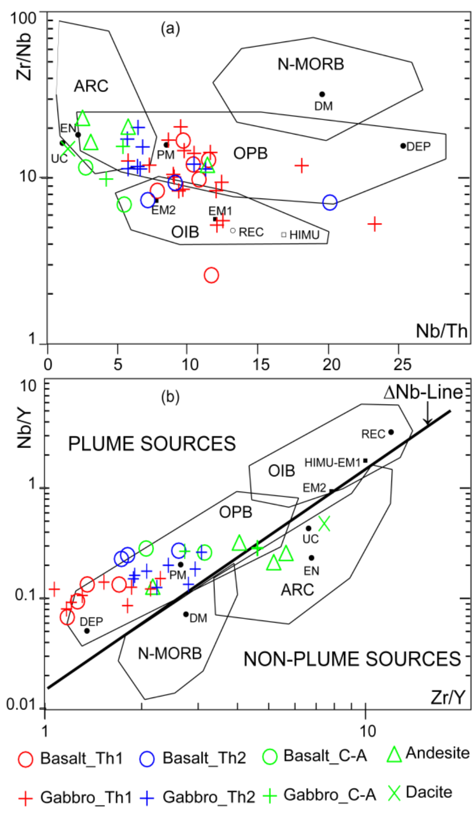

Figure 11: Plot of the ratios: (a) Zr/Nb vs. Nb/Th, and (b) Nb/Y vs. Zr/Y for the Mako greenstone belt. ARC: arc related basalts; N-MORB: Normal mid-ocean ridge basalt; OIB: oceanic island basalt. Hypothetical mantle sources: DM = shallow depleted

https://doi.org/10.5194/egusphere-2025-814
Preprint. Discussion started: 11 April 2025

mantle; EN = enriched component; PM = primitive mantle; REC = recycling component; UC = upper continental crust; DEP = depleted plume component; HIMU = high (U/Pb) source; EM1 and EM2 = enriched mantle sources (modified after Condie, 2003, 2005).

5.3 Evolutive model for the Mako greenstone belt

According to the trace element and isotopic data from the Mako greenstone belt, we have defined three magmatic series, including two different tholeiitic and one calc-alkaline series. Field relationships allow us to establish a relative chronological order from a first tholeiitic series, then a second tholeiitic series, and finally a calc-alkaline series. Their variability in composition suggests that these magmatic rocks were emplaced in different tectonic settings, and associated with different mantle sources (e.g., **Fig. 11**).

Considering a uniformitarian view for the Precambrian tectonic processes (e.g., Windley et al., 2021), the following evolutive model for the Mako greenstone belt can be proposed: i) *phase-A* started by the opening of an oceanic basin during the early Paleoproterozoic, which can be supported by some occurrences of MORB in the entire WAC, including the Mako greenstone belt (e.g., Zonou, 1987; Ngom et al., 2007; Theveniaut et al., 2010); ii) *phase-B* with the emplacement of a mantle plume in an intra-oceanic plate, triggering the formation on an oceanic plateau. The geochemical characteristics displayed by the tholeiitic series 1 witness the preservation of at least a part of the plume (e.g., Sproule et al., 2002; Condie 2003, 2005). A mantle plume emplacement has been previously proposed (Abouchami et al., 1990; Boher et al., 1992; Pawlig et al., 2006; Ngom et al., 2010; Augustin and Gaboury, 2017) for some Paleoproterozoic greenstone belts in WAC, including a recent study in Ghana (Agra et al., 2023), as well as in the Guiana Shield (Velásquez et. al., 2011; Borges et al., 2021); iii) *phase-C* with the initiation of an intra-oceanic subduction at or near to the mid-ocean ridge axis (e.g., Barth et al., 2008) and close to the oceanic plateau. During the earliest stages of subduction, the mantle plume could be still active and its interaction with the subduction-modified lithospheric magma and/or fluids derived from the slab could have generated a tholeiitic magma with chemical signatures like those found in the tholeiitic series 2, which differ from tholeiitic series 1 mainly for its slight negative Nb anomaly. Thus, tholeiitic rocks of series 2 could be also contributed to the building of the oceanic plateau; however, these rocks formed during the initial stages of island arc formation and have a slab-contaminated mantle source; iv) *phase-D* during the evolution of subduction processes and the maturation of the island arc, the calc-alkaline series were emplaced, as previously proposed in the WAC (e.g., Ama Salah et al., 1996; Béziat et al., 2000; Diallo, 2001; Ngom et al., 2007; Dioh et al., 2009). The subsequent maturation of the island arc may lead to the formation of more evolved calc-alkaline rocks and the emplacement of granitoid rocks (Vidal et al., 1996; Dia et al., 1997; Gueye et al., 2007; Parra-Avila et al., 2016).

The proposed evolution would have continued with a more-evolved subduction stage, where an oceanic lithosphere subducted beneath a continental plate, generating calc-alkaline magmatism, characteristic of a continental arc setting (e.g., Parra-Avila et al., 2019 and the references therein). Finally, the accretion of diverse Paleoproterozoic oceanic components, including MORB, OPB, and ARC, occurred against the Kenema-Man Archean domain during the Eburnean orogenesis (Kouamelan et al., 1997; Pitra et al., 2010; Eglinger et al., 2017; Koffi et al., 2022, 2023). This accretion is associated with the emplacement of a new generation of granitoid plutons (~ 2.20 – 2.16 Ga; Vidal et al., 1996; Dia et al., 1997;

https://doi.org/10.5194/egusphere-2025-814
Preprint. Discussion started: 11 April 2025

Gueye et al., 2007). In the Kedougou Kenieba Inlier, the shear zones found along the contacts between the originally deep-seated UM rocks and more superficial sedimentary and volcanic series suggest tectonic emplacement of UM bodies.

Studies on Birimian magmatism in the WAC at a regional scale include the work of Feybesse and Milési (1994), who examined the broader paleogeographic and geodynamic context, followed by more recent research by Grenholm et al. (2019), which proposes an evolutionary model for the Eburnean orogen within the Baoulé-Mossi domain. These authors conclude that the Eburnean orogen evolution would have occurred in a paleogeographic setting comparable to modern orogenic systems, with presence of accretionary and collisional domains, composed by several arcs and adjacent marginal basins (e.g., the region around Southeast Asia and the western Pacific; Grenholm et al., 2019). For the Eburnean orogen, it is interpreted as having gradually evolved into a continental environment due to a series of complex collisions between continental arcs and blocks.

We agree with the general idea that the construction of the Eburnean orogen took place mainly in a context of island arc followed by collision; however, our study deals with the stage prior to the "island arc" system, i.e., an oceanic plateau emplacement. Even if previous work (e.g. Abouchami et al., 1990; Lompo, 2009; Ngom et al., 2010; Augustin and Gaboury, 2017; Hayman et al., 2023) have considered that the contribution of oceanic plateau cannot be excluded for the Birimian crust growth, these have not been included in crustal growth models, except for a recent contribution from Ghana (Agra et al., 2023). In the Mako greenstone belt, we have shown that the tholeiitic rocks have isotopic signatures that reveal no continental influence in their formation. Finally, we consider that the oceanic plateau recognized in the Mako greenstone belt could also have contributed to Birimian crustal growth, during its accretion to the continental crust by some collisional episodes.

6 Conclusion

The geochemical and isotopic data of the Paleoproterozoic mafic and UM series of the Mako greenstone belt has revealed new evidence on the nature of the constituent formations and has led us to revisit the tectonic and geodynamic evolution of the belt. Based on geochemical (mainly REE and HFSE) and isotopic data, it has been possible: i) to recognize the two tholeiitic series (1 and 2) and one calc-alkaline series. The former consists of cumulative ultramafic rocks, basalts and gabbros, displaying juvenile signatures with positive εNd values (2.1 Ga); ii) to evidence that these series have been generated from different mantle sources into diverse geodynamic environments. Initially, an oceanic plateau emplaced in an intra-oceanic plate, triggered the formation of tholeiites 1 from a mantle plume source. Then, the same mantle plume became contaminated by subduction-modified lithospheric magmas and/or fluids derived from the slab, will be involved in the formation of the tholeiites 2 at the earliest stages of the arc built. This evolution will end with the maturation of the island arc, where the calc-alkaline series was emplaced; iii) to highlight, by comparison with data from other places of the WAC, the heterogeneity of the Birimian crust on a regional scale, leading to the coexistence within the West African Craton of series formed in different geodynamic contexts and finally geographically related by tectonic accretion process (Polat et al., 1998; Grenholm et al., 2019).

https://doi.org/10.5194/egusphere-2025-814
Preprint. Discussion started: 11 April 2025

Author contribution: M.B., L.B., D.B., P.D., I.L., P-M.N.: **Conceptualization**; I.L., M.B., L.B.: **Methodology**; I.L., M.B., L.B., D.B.: **Formal analysis**; I.L., D.D., P.D., G.V.: **Visualization**; M.B., L.B., D.B.: **Resources**; I.L., D.B., P.D., M.B., L.B., G.V.: **Writing - Original Draft**; D.B., P.D., P-M.N.: **Validation**; D.B., G.V., I.L., M.B., L.B.: **Writing - Review & Editing**.

Declaration of competing interest: The authors declare no competing interests. The authors have no relevant financial or non-financial interests to disclose.

Acknowledgments

We wish to gratefully acknowledge AMIRA International and the industry sponsors for their support of the WAXI project (P934B). Partial financial support was received from the West African Exploration Initiative (WAXI) project (P934B) and the Cultural Action Cooperation Service of the French Embassy in Senegal. We are also appreciative of the contribution of the various geological surveys department of mines in West Africa as sponsors in kind of WAXI. We thank the Cultural Action Cooperation Service which awarded to I.L. the PhD co-tutelle fellowship for 12 months of stay in France, with a financial support for analytical work. G.V. stay at GET has been supported through the grant EUR TESS no. ANR-18-EURE-0018 in the framework of the Programme des Investissements d'Avenir. We are grateful to F. De Parseval (thin sections preparations at the Géosciences Environnement Toulouse Laboratory); P. de Parseval and S. Gouy (EPM analyses at the Centre de microcaractérisation CASTAING, Université Toulouse); S. Mandrou (TIMS analyses at the Géosciences Environnement Toulouse Laboratory) for their technical assistance, as well as to A-M Cousin for the color drawing of the BKK map and geological section.

References

Abouchami, W., Boher, M., Michard, A., and Albarede, F.: A major 2.1 Ga old event of mafic magmatism in West Africa: an early stage of crustal accretion, Geophys. Res. Lett., 95, 17605–17629, 1990.

Agra, N. A., Elburg, M. A., and Vorster, C.: Constraints on Paleoproterozoic crustal growth from Birimian Supergroup lavas of the Bui belt (Ghana) in the West African Craton, Precambrian Res., 384, 106926, https://doi.org/10.1016/j.precamres.2022.106926, 2023.

Allibone, A., Lawrence, D., Scott, J., Fanning, M., Lambert-Smith, J., Stenhouse, P., Harbidge, R., Vargas, C., Turnbull, R., and Holliday, J.: Paleoproterozoic Gold Deposits of the Loulo District, Western Mali., in: Geology of the World's Major Gold Deposits and Provinces, Society of Economic Geologists, 141–162, 2020.

Alric, G.: Géochimie du volcanisme Birimien (Protérozoïque inferieur) de l'unité de la Haute-Comoé: N-E de la Côte d'Ivoire: premiers résultats, J. Afr. Earth Sci., 10, 669–681, 1990.

Alt, J.C., Shanks, W.C., and III Jackson, M. C.: Cycling of sulfur in subduction zones: the geochemistry of sulfur in the Mariana island arc and back-arc trough, Earth Planet. Sci. Lett., 119, 477–494, 1993.

https://doi.org/10.5194/egusphere-2025-814
Preprint. Discussion started: 11 April 2025

Ama-Salah, I., Liégeois, J., and Pouclet, A.: Evolution d'un arc insulaire océanique birimien précoce au Liptako nigérien (Sirba): géologie, géochronologie et géochimie, J. Afr. Sci., 22, 235–254, 1996.

Augustin, J., and Gaboury, D.: Paleoproterozoic plume-related basaltic rocks in the Mana gold district in western Burkina Faso, West Africa: Implications for exploration and the source of gold in orogenic deposits, J. Afr. Earth Sci., 129, 17–30, 2017.

Attoh, K., Evans, M.J., and Bickford, M.E.: Geochemistry of an ultramafic-rodingite rock association in the Paleoproterozoic Dixcove greenstone belt, southwestern Ghana, J. Afr. Earth Sci., 45, 333–346, https://doi.org/10.1016/j.jafrearsci.2006.03.010, 2006.

Bach, W., and Erzinger, J.: Volatile components in basalts and basaltic glasses from the EPR at 9 degre 30 N, Proc. Odp. Sci. results, 142, 23–29, 1995.

Baratoux, L., Metelka, V., Naba, S., Jessell, M.W., Grégoire, M., and Ganne, J.: Juvenile Paleoproterozoic crust evolution during the Eburnean Orogeny (2.2-2.0 Ga), Western Burkina Faso, Precambrian Res., 191, 18–45, doi:10.1016/j.precamres.2011.08.010, 2011.

Barrat, I.A., Zanda, B., Jambon, A., and Bollinger, C.: The lithophile trace elements in enstatite chondrites, Geochim. Cosmochim. Acta, 128, 71–94, 2014.

Barth, M. G., Mason, P. R. D., Davies, G. R., and Drury, M. R.: The Othris Ophiolite, Greece: A snapshot of subduction initiation at a mid-ocean ridge, Lithos, 100, 234–254, 2008.

Bassot, J. P.: Le complexe volcano-plutonique calcoalcalin de la rivère Daléma (Est Sénegal): discussion de sa signification géodynamique dans le cadre de l'orogénèse éburnéenne (Protérozoïque inférieur), J. Afr. Earth Sci., 6, 505–519, 1987.

Bassot, J. P.: Etude géologique du Sénégal oriental et de ses confins Guinéo Maliens, Mémoire BRGM No. 40, 1966.

Bassot, J. P., and Dommanget, A.: Mise en évidence d'un accident majeur affectant le Protérozoïque inférieur des confins Sénégalo-maliens. Compt. Rend. Acad. Sci. Paris, T. 302, Série II, N° 17, 1101–1106, 1986.

Batiza, R., Niu, Y., Karsten, J. L., Boger, W., Potts, E., Norby, L., and Butler, R.: Steady and non-steady state magma chambers below the East Pacific rise, Geophys. Res. Lett., 23, 221–224, https://doi.org/10.1029/95GL00016, 1996.

Ben Othman, Allegre, D., and Claude, J.: U-Th systematics at 13 degree N East Pacific ridge segment, Earth Planet. Sci. Lett., 98, 129–137, 1990.

Bessoles, B.: Géologie de l'Afrique. Le craton ouest- africain, Mémoire BRGM, Paris, 88 p, 1977.

Béziat, D., Bourges, F., Debat, P., Lompo, M., Martin, F., and Tollon, F.: A Paleoproterozoic ultramafic-mafic assemblage and associated volcanic rocks of the Boromo greenstone belt: fractionates originating from island-arc volcanic activity in the West African craton, Precambrian Res., 101, 25–47, 2000.

Block, S., Ganne, J., Baratoux, L., Zeh, A., Parra-Avila, L. A., Jessell, M., Ailleres, L., and Siebenaller, L.: Petrological and geochronological constraints on lower crust exhumation during Paleoproterozoic (Eburnean) orogeny, NW Ghana, West African Craton, J. Metamorph. Geol., 33, 463–494, https://doi.org/10.1111/jmg.12129, 2015.

Block, S., Baratoux, L., Zeh, A., Laurent, O., Bruguier, O., Jessell, M., Ailleres, L., Sagna, R., Parra-Avila, L. A., and Bosch, D.: Paleoproterozoic juvenile crust formation and stabilisation in the south-eastern West African Craton (Ghana); new insights from UPb-Hf zircon data and geochemistry, Precambrian Res., 287, 1–30, 2016.

Bloomer, S. H., and Hawkins, J. W. JR.: Petrology and Geochemistry of Boninite series volcanic rocks from the Mariana trench, Contrib. Miner. Pet., 97, 361–377, 1987.
Bloomer, S. H., Stern, R. J., Fisk, E., and Geschwind, C. H.: Shoshinitic Volcanism in The Northern Mariana arc: 1. Mineralogic and major and trace element characteristics, J. Geophys. Res., B94, 4469–4496, 1989.
Boher, M., Abouchami, W., Michard, A., Albarede, F., and Arndt, N. T.: Crustal growth in West Africa at 2.1 Ga, J. Geophys. Res., 97, 345–369, https://doi.org/10.1029/91JB01640, 1992.
Bonhomme, M.: Contribution à l'étude géochronologique de la plate-forme de l'Ouest africain, Ann. Fac. Sci. N°. 5, Univ. Clermont-Ferrand, 1962.
Borges, C.C.A., Toledo, C.L.B., Silva, A.M., Kirk, J., Ruiz, J., Chemale, F., Souza, R.G., Santos, B.A., Campos, M.P., Campos, L.M., and Santos, A.M.: Archean to Paleoproterozoic evolution of the Crixás greenstone belt, Central Brazil: Insights from two contrasting assemblies of metaigneous rocks, Lithos, 404–405, 106493. https://doi.org/10.1016/j.lithos. 2021.106493, 2021.
Byers, C. D., Garcia, M. O., and Muenow, D. W.: Volatiles in basaltic glasses from the East Pacific Rise at 218N: implications for MORB sources and submarine lava flow morphology, Earth Planet. Sci. Lett., 79, 9–20, 1986.
Castaing, C., Billa, M., Milesi, J. P., Thiéblemont, D., Le Metour, J., Egal, E., Donzeau, M., (BRGM), Guerrot, C., Cocherie, A., Chevremont, P., Tegyey, M., Itard, Y., (BRGM), Zida, B., Ouédraogo, I., Koté, S., Kaboré, B.E., Ouédraogo, C. (Bumigeb), Ki, J.C., and Zunino, C. (Antea): Notice explicative de la Carte géologique et minière du Burkina Faso à 1/1 000 000, 2003.
Castillo, P. R., Klein, E., Bender, J., Langmuir, C., Shirey, S., Batiza, R., and White, W.: Petrology and Sr, Nd, and Pb isotope geochemistry of mid-ocean ridge basalt glasses from the 11°45′N to 15°00′N segment of the East Pacific Rise, Geochem. Geophys. Geosyst., 1, 1011, https://doi.org/10.1029/1999GC000024, 2000.
Cissokho, S.: Etude géologique du secteur de Mako (partie méridionale du super-groupe de Mako, boutonnière de Kédougou-Kéniéba, Sénégal oriental) : implications sur la diversité magmatique, Thèse de doctorat 3[ème] cycle Univ. Cheikh Anta Diop, Dakar, Sénégal, 212 p, 2010.
Cohen, R. S., Evensen, N. M., Hamilton, P. J., and O'nions, R. K.: U-Pb, Sm-Nd and Rb-Sr systematics of mid-ocean ridge basalt glasses, Nature, 283, 149–153, 1980.
Condie, K. C.: High field strength element ratios in Archean basalts: a window to evolving sources of mantle plumes?, Lithos, 79, 491–504, doi:10.1016/j.lithos.2004.09.014, 2005.
Condie, K. C.: Incompatible element ratios in oceanic basalts and komatiites: tracking deep mantle sources and continental growth rates with time, Geochem. Geophys. Geosys. (G3), 4 (1), 1005, doi:10.1029/2002GC000333, 2003.
Condie, K. C.: Archean crustal evolution In: Windley, B.F. (Ed.). Dev, Precambrian Geol., 528 p, 1994.
Dabo, M., Aïfa, T., Gassama, I., and Ngom, P. M.: Thrust to transpression and transtension tectonics during the Paleoproterozoic evolution of the Birimian Greenstone Belt of Mako, Kédougou-Kéniéba Inlier, eastern Senegal, J. Afr. Earth Sci., 148, 14–29, https://doi.org/10.1016/j.jafrearsci.2018.05.010, 2018.
Dabo, M., Aïfa, T., Gning, I., Faye, M., Ba, M. F., and Ngom, P. M.: Lithological architecture and petrography of the Mako Birimian greenstone belt, Kédougou-Kéniéba Inlier, eastern Senegal, J. Afr. Earth Sci., 131, 128–144, http://dx.doi.org/10.1016/j.jafrearsci.2017.04.005, 2017.
Dampare, S., Shibata, T., Asiedu, D., Okono, O., Manu, J., and Sakyi, P.: Sr-Nd isotopic compositions of Paleoproterozoic metavolcanic rocks from the southern Ashanti volcanic belt, Ghana, Earth Sci. Rep., 16, 9–28, 2009.

Dampare, S.B., Shibata, T., Asiedu, D.K., Okano, O., Osae, S.K.D., Atta-Peters, D., and Sakyi, P.A.: Ultramafic–mafic and granitoids supra-subduction magmatism in the southern Ashanti volcanic belt, Ghana: evidence from geochemistry and Nd isotopes, Geol. J., 1–37, https://doi.org/10.1002/gj.3512, 2019.

Dampare, S. B., Shibata, T., Asiedu, D. K., Osae, S., and Banoeng-Yakubo, B.: Geochemistry of Paleoproterozoic metavolcanic rocks from the southern Ashanti volcanic belt, Ghana: petrogenetic and tectonic setting implications, Precambrian Res., 162, 403–423, https://doi.org/10.1016/j.precamres.2007.10.001, https://doi.org/10.1016/j.precamres.2007.10.001, 2008.

De Kock, G. S., Armstrong, R. A., Siegfried, H. P., and Thomas, E.: Geochronology of the Birim Supergroup of the West African craton in the Wa-Bolé region of west-central Ghana: implications for the stratigraphic framework, J. Afr. Earth Sci., 59, 1–40, https://doi.org/10.1016/j.jafrearsci.2010.08.00, 2011.

Debat, P., Diallo, D.P., Ngom, P.M., Rollet, M., and Seyler, M.: La série de Mako dans ses parties centrale et méridionale (Sénégal Oriental, Afrique de l'ouest). Précisions sur l'évolution de la série volcanosédimentaire et données géochimiques préliminaires sur les formations magmatiques post-tectoniques, J. Afr. Earth Sci., 2, 71–79, https://doi.org/10.1016/0899-5362 (84) 90023-X, 1984.

Debat, P., Nikiéma, S., Mercier, A., Lompo, M., Béziat, D., Bourges, F., Roddaz, M., Salvi, S., Tollon, F., and Wenmenga, U.: A new metamorphic constraint for the Eburnean orogeny from Paleoproterozoic formations of the Man shield (Aribinda and Tampelga countries, Burkina Faso), Precambrian Res., 123, 47–65, doi:10.1016/S0301-9268(03)00046-9, 2003.

DePaolo, D. J.: Neodymium Isotope Geochemistry, Minerals and Rocks, Springer Berlin Heidelberg, https://doi.org/10.1007/978-3-642-48916-7, 1988.

DePaolo, D. J., and Wasserburg, G. J.: Nd isotopic variations and petrogenetic models, Geophys. Res. Lett., 3, 249–252, https://doi.org/10.1029/GL003i005p00249, 1976.

Dia, A.: Caractère et signification des complexes magmatiques et métamorphiques du secteur de Sandikounda-Laminia (Nord de la boutonnière de Kédougou, Est du Sénégal): un modèle géodynamique du Birimien de l'Afrique de l'Ouest, Thèse de doctorat d'état Univ. Cheikh Anta Diop de Dakar, Sénégal. 350 p, 1988.

Dia, A., Van Schmus, W. R., and Kröner, A.: Isotopic constraints on the age and formation of a Paleoproterozoic volcanic arc complex in the Kedougou Inlier, eastern Senegal. West Africa, J. Afr. Earth Sci., 24, 197–213, 1997.

Diallo, D. P.: Le paléovolcanisme de la bordure occidentale de la boutonnière de Kédougou, Paléoprotérozoïque du Sénégal oriental : incidences géotectoniques, J. Afr. Earth Sci., 32, 919–940, 2001.

Diallo, D. P.: Caractérisation d'une portion de croûte d'âge protérozoïque inférieur du craton Ouest-africain : cas de l'encaissant des granitoïdes dans le super-groupe de Mako (boutonnière de Kédougou). Implications géodynamiques, Thèse de doctorat d'état Université Cheikh Anta Diop, Dakar, Sénégal, 466 p, 1994.

Diallo, D. P.: Contribution à l'étude géologique de la série du Dialé (Birimien) dans les monts Bassaris-Sénégal oriental (secteur de Bandafassi-Ibel-Ndébou-Landiéné). Thèse de 3éme cycle Université Cheikh Anta Diop, Dakar, Sénégal, 181 p, 1983.

Diallo, M., Baratoux, L., Dufréchou, G., Jessell, M. W., Vanderhaeghe, O., Ly, S., and Baratoux, D.: Structure of the Paleoproterozoic Kédougou-Kéniéba Inlier (Senegal-Mali) deduced from gravity and aeromagnetic data, J. Afr. Earth Sci., 162, 103732, 2020.

Diatta, F., Ndiaye, P. M., Diene, M., Amponsah, P. O., and Ganne, J.: The structural evolution of the Dialé-Daléma basin, Kédougou-Kéniéba Inlier, Eastern Senegal, J. Afr. Earth Sci., 129, 923–933, https://doi.org/10.1016/j.jafrearsci.2017.02.033, 2017.

Diene, M., Fullgraf, T., Diatta, F., Gloaguen, E., Gueye, M., and Ndiaye, P. M.: Review of the Senegalo-Malian shear zone system - timing, kinematics and implications for possible Au mineralisation styles, J. Afr. Earth Sci., 112, 485–504, https://doi.org/10.1016/j.jafrearsci.2015.05.004, 2015.

Diene, M., Gueye, M., Diallo, D.P., and Dia, A.: Structural evolution of a Precambrian Segment: example of the Paleoproterozoic formations of the Mako belt (Eastern Senegal, West Africa), Int. J. Geosci., 03, 153–165, doi:10.4236/ijg.2012.31017, 2012.

Dioh, E.: Caractérisation, signification et origine des formations birimiennes encaissantes du granite de Dioumbalou (Partie septentrionale de la boutonnière de Kédougou-Sénégal oriental), Thèse de doctorat d'état Univ. Cheikh Anta Diop, Dakar, Sénégal, 425 p, 1995.

Dioh, E.: Etude des roches magmatiques Birimiennes de la région de Sonfara- Laminia- Médina Foulbé (Sénégal oriental), Thèse de doctorat 3ème cycle Université Nancy I, France, 144 p, 1986.

Dioh, E., Béziat, D., Debat, P., Grégoire, M., and Ngom, P. M.: Diversity of the Palaeoproterozoic granitoids of the Kédougou inlier (eastern Sénégal): petrographical and geochemical constraints, J. Afr. Earth Sci., 44, 351–371, doi:10.1016/j.jafrearsci.2005.11.024, 2006.

Dioh, E., Béziat, D., Grégoire, M., and Debat, P.: Origin of rare earth element variations in clinopyroxene from plutonic and associated volcanic rocks from the Foulde basin, Northern Kedougou inlier, Senegal, West Africa, Eur. J. Mineral, 21, 1029–1043, https://doi.org/10.1127/0935-1221/2009/0021-1963, 2009.

Dioh, E., Debat, P., Dia, A., Pons, J., Rocci, G., and Rollet, M.: Caractérisation d'un complexe rubané dans les formations Birimiennes de la partie septentrionale de la boutonnière de Kédougou - Kéniéba, C. R. Acad. Sci. Paris, Sér. 2, 310, 935–940, 1990.

Doumbia, S., Pouclet, A., Kouamelan, A., Peucat, J.J., Vidal, M., and Delor, C.: Petrogenesis of juvenile-type Birimian (Paleoproterozoic) granitoids in Central Côte-d'Ivoire, West Africa: geochemistry and geochronology, Precambrian Res., 87, 33–63, https://doi.org/10.1016/S0301-9268(97)00201-5, 1998.

Eglinger, A., Thébaud, N., Zeh, A., Davis, J., Miller, J., Parra-Avila, L. A., Loucks, R., McCuaig, C., and Belousova, E.: New insights into the crustal growth of the Paleoproterozoic margin of the Archean Kéména-Man domain, West African craton (Guinea): Implications for gold mineral system, Precambrian Res., 292, 258–289, https://doi.org/10.1016/j.precamres.2016.11.012, 2017.

Elliott, T.R., Plank, T., Zindler, A., White, W., and Bourdon, B.: Element transport from slab to volcanic front at the Mariana arc, J. Geophys. Res., B102, 14991–15019, 1997.

Feybesse, J. L., and Milési, J. P.: The Archaean/Proterozoic contact zone in West Africa: a mountain belt of décollement thrusting and folding on a continental margin related to 2.1 Ga convergence of Archaean cratons, Precambrian Res., 69, 199–227, 1994.

Furnes, H., Dilek, Y., and De Wit, M.: Precambrian greenstone sequences represent different ophiolite types, Gondwana Res., 27, 649–685, https://doi.org/10.1016/j.gr.2013.06.004, 2015.

https://doi.org/10.5194/egusphere-2025-814
Preprint. Discussion started: 11 April 2025

Ganne, J., De Andrade, V., Weinberg, N., Dubacq, B., Vidal, O., Kagambega, N., Naba, S., Baratoux, L., Jessell, M., and Allibone, J.: Modern-style plate subduction pre-served in the Palaeoproterozoic West African craton, Nat. Geosci., 5, 60–65, 2012.

Ganne, J., Gerbault, M., and Block, S.: Thermo-mechanical modeling of lower crust exhumation-constraints from the metamorphic record of the Palaeoproterozoic Eburnean orogeny, West African craton, Precambrian Res., 243, 88–109, https://doi.org/10.1016/j.precamres.2013.12.016, 2014.

Gasquet, D., Barbey, P., Adou, M., and Paquette, J.: Structure, Sr-Nd isotope geochemistry and zircon U-Pb geochronology of the granitoids of the Dabakala area (Côte d'Ivoire): evidence for a 2.3 Ga crustal growth event in the Palaeoproterozoic of West Africa, Precambrian Res., 127, 329–354, https://doi.org/10.1016/S0301-9268(03)00209-2, 2003.

Gozo, A.: Pétrologie du volcanisme paléoprotérozoïque calco-alcalin du groupe de Mako (Sénégal Oriental) : incidences géotectoniques, Thèse de doctorat unique Université Cheikh Anta Diop, Dakar, Sénégal, 182 p, 2017.

Gozo, A., Diene, M., Diallo, D. P., Dioh, E., Gueye, M., and Ndiaye, P. M.: Petrological and structural approach to understanding the mechanism of formation and development of paleoproterozoic calc-Alkaline volcanic rocks of West Africa's Craton: an example of the Mako and Foulde groups (Kedougou Inlier in Eastern Senegal), Int. J. Geosci., 6, 675–691, 2015.

Grenholm, M., Jessell, M., and Thébaud, N.: A geodynamic model for the Paleoproterozoic (2.27 -1.96 Ga) Birimian Orogen of the southern West African Craton-insights into an evolving accretionary-collisional orogenic system, Earth Sci. Rev., 192, 138–193, 2019.

Gribble, R. F., Stern, R. J., Bloomer, S. H., Stüben, D., Ôhearn, T., and Newman, S.: MORB mantle and subduction components interact to generate basalts in the Southern Mariana trough back-arc basin, Geochim. Cosmochim. Acta, 60, 2153–2166, 1996.

Gribble, R. F., Stern, R. J., Newman, S., Bloomer, S. H., and O'Hearn, T.: Chemical and isotopic composition of lavas from the Northern Mariana trough: implications for magmagenesis in back-arc basins, J. Petrol., 39, 125–154, 1998.

Gueye, M., Ngom, P. M., Diène, M., Thiam, Y., Siegesmund, S., Wemmer, K., and Pawlig, S.: Intrusive rocks and tectono-metamorphic evolution of the Mako Paleoproterozoic belt (Eastern Senegal, West Africa), J. Afr. Earth Sci., 50, 88–110, https://doi.org/10.1016/j.jafrearsci.2007.09.013, 2008.

Gueye, M., Siegesmund, S., Wemmer, K., Pawlig, S., Drobe, M., and Notle, N.: New evidences for an Early Birimian evolution in the West African Craton: an example from the Kedougou Kenieba inlier, SE- Senegal, South Afr. J. Geol., 110, 179–190, 2007.

Hawkins, J. W., Lonsdale, P. F., Macdougall, J. D., and Volpe, A. M.: Petrology of the axial ridge of the Mariana Trough backarc spreading center, Earth Planet. Sci. Lett., 100, 226–250, 1990.

Hawkins, J. W., and Melchior, J. T.: Petrology of Mariana trough and Lau basin basalts, J. Geophys. Res., 90, 11431–11468, 1985.

Hayman, P. C., Bolz, P., Senyah, G., Tegan, E., Denyszyn, S., Murphy, D. T., and Jessell, M. W.: Physical and geochemical reconstruction of 2.35 – 2.1 Ga volcanic arc (Toumodi Greenstone Belt, Ivory Coast, West Africa, Precambrian Res., 389, 107029, 2023.

Hekinian, R., Thompson, G., and Bideau, R. D.: Axial and off-axial heterogeneity of basaltic rocks from the east Pacific rise at 12 degree 35 ÕN-12 degree 51 ÕN, J. Geophys. Res., 94, 17437–17463, 1989.

Hickey, R. L., and Frey, F. A.: Rare-Earth Element geochemistry of Mariana fore-arc volcanics deep sea drilling project site 458 and hole 459b, Init. Rep. Deep Sea Drill Proj., 60, 735–742, 1982.

Hickey-Vargas, R.: Origin of the Indian Ocean-type isotopic signature in basalts from Philippine Sea plate spreading centers: An assessment of local versus large-scale processes, J. Geophys. Res. Solid. Earth, 103, 20963–20979, 1998.

Hickey-Vargas, R.: Isotope characteristics of submarine lavas from the Philippine sea: Implications for the origin of arc and basin magmas of the Philippine tectonic plate, Earth Planet. Sci. Lett., 107, 290–304, 1991.

Hofmann, A. W., and White, W. M.: Ba, Rb and Cs in the Earth's Mantle, Zeitschr Naturforsch, 38A, 256–266, 1983.

Hollings, P., and Kerrich, R.: Geochemical systematics of tholeiites from 2.86 Ga Pickle Crow Assemblage, northwestern Ontario: arc basalts with positive and negative Nb-Hf anomalies, Precambrian Res., 134, 1–20, 2004.

Ikeda, Y., Nagao, K., Stern, R. J., Yuasa, M., and Newman, S.: Noble gases in pillow basalt glasses from the Northern Mariana trough back-arc basin, Isl. Acr., 7, 471–478, 1998.

Junner, N. R.: Notes on the classification of the Precambrian of West African, XIX Int. Geol. Cong. Algiers, No. 20, 1954.

Kitson, A. E.: Carte géologique provisoire de la Gold Coast et du Togo occidental, avec note explicative, Bull. Gold Coast Geol. Surv. Accra, No. 2, 1928.

Koffi, A. Y., Baratoux, L., Pitra, P., Kouamelan, A. N., Vanderhaeghe, O., Thébaud, N., Bruguier, O., Block, S., Fossou Kouadio, H. J. L., and Kone, J.: A tectonic model for the juxtaposition of granulite- and amphibolite-facies rocks in the Eburnean orogenic belt (Sassandra-Cavally domain, Côte d'Ivoire), BSGF - Earth Sci. Bull, 194, 11, https://doi.org/10.1051/bsgf/2023007, 2023.

Koffi, A. Y., Thébaud, N., Kouamelan, A. N., Baratoux, L., Bruguier, O., Vanderhaeghe, O., Pitra, P., Kemp, A. I. S., and Evans, N. J.: Archean to Paleoproterozoic crustal evolution in the Sassandra-Cavally domain (Côte d'Ivoire, West Africa): Insights from Hf and U-Pb zircon analyses, Precambrian Res., 382, 106875, https://doi.org/10.1016/j.precamres.2022.106875, 2022.

Kone, J., Vanderhaeghe, O., Diatta, F., Baratoux, L., Thebaud, N., Bruguier, O., Ndiaye, P. M., Duchene, S., Pitra, P., and Ganne, J.: Source and deposition age of the Dialé-Daléma metasedimentary series (Kédougou-Kéniéba Inlier, Senegal) constrained by U-Pb geochronology on detrital zircon grains, J. Afr. Earth Sci., 165, 103801, https://doi.org/10.1016/j.jafrearsci.2020.103801, 2020.

Kouamelan, A. N., Kra, K. S. A., Djro, S. C., Paquette, J. L., and Peucat, J. J.: The Logoualé band: a large Archean crustal block in the Kenema-Man domain (Man-Leo rise, West African craton) remobilized during Eburnean orogeny (2.05 Ga), J. Afr. Earth Sci., 148, 6–13, https://doi.org/10.1016/j.jafrearsci.2017.09.004, 2018.

Kouamelan, A. N., Peucat, J. J., and Delor, C.: Reliques archéennes (3.15 Ga) au sein du magmatisme birimien (2.1 Ga) de Côte d'lvoire, Craton Ouest-Africain, C. R. Acad. Sci. Paris, 324, 716–727, 1997a.

Labou, I.: Les complexes mafiques et ultramafiques birimiens de la ceinture de Mako (Sénégal oriental) témoins d'un domaine intra-océanique vers un domaine d'arc insulaire, Thèse de doctorat en cotutelle Université Toulouse III Paul Sabatier (France) et Université Cheikh Anta Diop de Dakar (Sénégal), 329 p, 2019.

Labou, I., Benoit, M., Baratoux, L., Grégoire, M., Ndiaye, P. M., Thebaud, N., Béziat, D., and Debat, P.: Petrological and geochemical study of Birimian ultramafic rocks within the West African Craton: Insights from Mako (Senegal) and Loraboué (Burkina Faso) lherzolite/harzburgite/wehrlite associations, J. Afr. Earth Sci., 162, 103677, https://doi.org/10.1016/j.jafrearsci.2019.103677, 2020.

Lambert-Smith, J. S., Lawrence, D. M., Müller, W., and Treloar, P. J.: Palaeotectonic setting of the south-eastern Kédougou-Kéniéba Inlier, West Africa: new insights from igneous trace element geochemistry and U-Pb zircon ages, Precambrian Res., 274, 110–135, https://doi.org/10.1016/j.precamres.2015.10.013, 2016.

Lawrence, D. M., Treloar, P. J., Rankin, A. H., Harbidge, P., and Holliday, J.: The geology and mineralogy of the Loulo mining district, Mali, West Africa: evidence for two distinct styles of orogenic gold mineralization, Econ. Geol., 108, 199–227, https://doi.org/10.2113/econgeo.108.2.199, 2013.

Leake, B.E., Woolley, A.R., Birch, W.D., Burke, E.A.J., Ferraris, G., Grice, J.D., Hawthorne, F.C., Kisch, H.J., Krivovichev, V. G., Schumacher, J. C., Stephenson, N. C. N., and Whittaker, E. J. W.: Nomenclature of amphiboles: additions and revisions to the International Mineralogical Association's amphibole nomenclature, Can Miner., 41, 1355-1370, 2003.

Ledru, P., Pons, J., Milesi, J. P., Feybesse, J. L., Dommanget, A., Johan, V., Diallo, M., and Vinchon, C.: Tectonique transcurrente et évolution polycyclique dans le Birimien, Protérozoïque inférieur du Sénégal-Mali (Afrique de l'Ouest), C.R. Acad. Sci. Paris, T. 308 Sér. II, 117–122, 1989.

Ledru, P., Pons, J., Milesi, J., Feybesse, J., and Johan, V.: Transcurrent tectonics and polycyclic evolution in the Lower Proterozoic of Senegal-Mali, Precambrian Res., 50, 337–354, 1991.

Leube, A., Hirdes, W., Mauer, R., and Kesse, G. O.: The Early Proterozoic Birimian Supergroup of Ghana and Some Aspects of its Associated Gold Mineralization, Precambrian Res., 46, 139–165, 1990.

Lin, P. N., Stern, R. J., and Bloomer, S. H.: Shoshinitic volcanism in the Northern Mariana arc: 2. Large Ion-Lithophile and Rare Earth Element abundances: evidence for the source of incompatible element enrichments in intra-oceanic arcs, J. Geophys. Res., B94, 4497–4514, 1989.

Loh, G., Hirdes, W., Anani, C., Davis, D. W., and Vetter. U. K.: Explanatory Notes for the Geological Map of Southwest Ghana 1:100,000 Sekondi (0402A) and Axim (0403B) Sheets, Geol. Surv. Bull., 49, 149, 1999.

Lompo, M.: Geodynamic evolution of the 2.25-2.0 Ga Palaeoproterozoic magmatic rocks in the Man-Leo Shield of the West African Craton. A model of subsidence of an oceanic plateau, Geol. Soc. Lond. Spec. Publ., 323, 231–254, 2009.

Macdougall, J. D., and Lugmair, G. W.: Sr and Nd isotopes in basalts from the east Pacific rise: significance for mantle heterogeneity, Earth Planet. Sci. Lett., 77, 273–284, 1986.

Mahoney, J. J., Sinton, J. M., Kurz, M. D., Macdougall, J. D., Spencer, K. J., and Lugmair, G. W.: Isotope and trace element characteristics of a super-fast spreading ridge: East Pacific Rise 13-23 degrees, Earth Planet. Sci. Lett., 121, 171–191, 1993.

Masurel, Q., Thébaud, N., Miller, J., Ulrich, S., Hein, K. A. A., Cameron, G., Béziat, D., Bruguier, O., and Davis, J. A.: Sadiola Hill: a world-class carbonate-hosted gold deposit in Mali, West Africa, Econ. Geol., 112, 23–47, 2017.

Meijer, A.: Pb and Sr isotopic data bearing on the origin of volcanic rocks from the Mariana island-arc system, Geol. Soc. Am. Bull., 87, 1358-1369, 1976.

https://doi.org/10.5194/egusphere-2025-814
Preprint. Discussion started: 11 April 2025

Meijer, A., and Reagan, M. K.: Petrology and geochemistry of the Island of Sarigan in the Mariana arc: calc-alkaline volcanism in an oceanic setting, Contrib. Miner. Pet., 77, 337–354, 1981.

Milesi, J. P., Dommanget, A., Johan, V., and Diallo, M.: Lower Proterozoïc succession in Senegal and Mali (West Africa): Position of sediment-hosted Au and Fe deposits of Loulo area and significance in terms of crustal evolution, Abstracts, 28th Int. Geol. Cong. Washington USA July, No. 9, 19, 2–3, 1989.

Milesi, J., Feybesse, J., Pinna, P., Deschamps, Y., Kampunzu, H., Muhongo, S., Lescuyer, J. L., Le Goff, E., Delor, C., Billa, M., Ralay, F., and Heinry, C.: Geological map of Africa 1:10000000 SIGAfrique project. In: 20th Conference of African Geology, BRGM, Orleans, France, 2-7 June, http://www.sigafrique.net (lastaccessed 14/12/2010), 2004.

Morimoto, N., Fabriés, J., Ferguson, A. K., Ginsburg, L. V., Ross, M., Seifert, F. A., Zussman, J., AoKi, K., and Gottardi, G.: Nomenclature of pyroxenes (subcommitee on pyroxene, IMA.), Mineral. Mag., 52, 535–550, 1988.

Moussolo, J. B.: Etude du volcanisme de Baniomba dans la partie méridionale du groupe de Mako: boutonnière de Kédougou-Kéniéba (Sénégal oriental), Mémoire DEA, Univ. Cheikh Anta Diop de Dakar, Sénégal, 74 p, 2000.

Natland, J. H.: Partial melting of a lithologically heterogeneous mantle: inferences from crystallization histories of magnesian abyssal tholeiites from the Siqueiros fracture zone, Geol. Soc. Spec. Pub., 42, 41–70, 1989.

Ndiaye, P. M., Dia, A., Vialette, Y., Diallo, D. P., Ngom, P. M., Sylla, M., Wade, S., and Dioh, E.: Données pétrographiques, géochimiques et géochronologiques nouvelles sur les granitoïdes du Paléoprotérozoïque du super-groupe de Dialé-Daléma (Sénégal oriental): implications pétrogénétiques et géodynamiques, J. Afr. Earth Sci., 25, 193–208, 1997.

Newman, S., Stolper, E., and Stern, R.: H_2O and CO_2 in magmas from the Mariana arc and back arc systems, Geochem. Geophys. Geosyst., 1, 1013, 2000.

Nui, Y., Collerson, K. D., Batiza, R., Wendt, J. I., and Regelous, M.: Origin of enriched-type mid-ocean ridge basalt at ridges far from mantle plumes: the East Pacific Rise at 11°20′N, J. Geophys. Res., 104, 7067–7087, 1999.

Ngom, P. M.: Caractérisation de la croûte Birimienne dans les parties centrale et méridionale du supergroupe de Mako. Implications géochimiques et pétrogénétiques, Thèse de doctorat d'état Université Cheikh Anta Diop, Dakar, Sénégal, 240 p, 1995.

Ngom, P. M.: Caractères géochimiques des formations Birimiennes du supergroupe de Mako (Sabodala et ses environs), Afr. Earth Sci., 8, 91–97, 1989.

Ngom, P. M.: Contribution à l'étude de la série Birimienne de Mako dans le secteur de Sabodala (Sénégal oriental), Thèse de 3éme cycle Université Nancy I, France, 134 p, 1985.

Ngom, P. M., Cissokho, S., Gueye, M., and Joron, J. L.: Diversité du volcanisme et évolution géodynamique au Paléoprotérozoïque : exemple du Birimien de la boutonnière de Kédougou-Kéniéba (Sénégal), Afr. Geosci. Rev., 18, 1–22, 2011.

Ngom, P. M., Cordani, U. G., Teixeira, W., and Janasi, V. A.: Sr and Nd isotopic geochemistry of the early ultramafic–mafic rocks of the Mako bimodal volcanic belt of the Kedougou-Kenieba inlier (Senegal), Arab. J. Geosci., 3, 49–57, DOI 10.1007/s12517-009-0051-3, 2010.

Ngom, P. M., Gueye, M., Cissokho, S., Joron, J. L., Treuil, M., and Dabo, M.: Signification géodynamique des roches volcaniques dans les ceintures de roches vertes d'âge paléoprotérozoïque; exemple de la partie méridionale du supergroupe de Mako, boutonnière de Kédougou (Sénégal). Approche des éléments en traces, J. Sci. Technol., 5, 52–71, 2007.

Ngom, P. M., Rocci, G., Debat, P., Dia, A., Diallo, D. P., Dioh, E., and Sylla, M.: Les massifs basiques et ultrabasiques Birimiens du supergroupe de Mako (Sénégal oriental): pétrographie, géochimie et signification pétrogénétique, Bull. L'IFAN Cheikh Anta Diop, Dakar, Sénégal, T.49, Sér. A, N° 2, 33–54, 1998.

Ouédraogo, A.: Etude de quelques unités plutoniques basiques éburnéennes dans le sillon de Bouroum Yalogo au NE du Burkina Faso, Thèse de doctorat 3$^{\text{ème}}$ cycle Université Nancy I, France, 64 p, 1985.

Parra Avila, L. A., Kemp, A. I. S., Fiorentini, M. L., Belousova, E., Baratoux, L., Block, S., Jessell, M., Davis, J., and McCuaig, T. C.: The geochronological evolution of the Paleoproterozoic Baoulé-Mossi domain of the southern West African Craton, Precambrian Res., 300, 1–27, 2017.

Pawlig, S., Gueye, M., Klischies, R., and Schwarz, S.: Geochemical and Sr – Nd isotopic data on Birimian formations of the Kedougou-Kénieba Inlier (Eastern Senegal): implications of the Paleoproterozoic evolution of the West African Craton, South Afr. J. Geol., 109, 407–423, 2006.

Peate, D. W., Pearce, J. A., Hawkesworth, C. J., Edwards, C. M. H., and Hirose, K.: Geochemical variations in Vanuatu arc lavas: the role of subducted material and a variable mantle wedge composition, J. Petrol., 38, 1331-1358, 1997.

Pickett, D. A., and Murrell, M. T.: Observations of $^{231}Pa/^{235}U$ disequilibrium in volcanic rocks, Earth Planet. Sci. Lett., 148, 259–271, https://doi.org/10.1016/S0012-821X(97)00037-X, 1997.

Pin, C., Briot, D., and Poitrasson, F.: Concomitant separation of strontium and samarium-neodymium for isotopic analysis in silicate samples, based on specific extraction chromatography, Anal. Chim. Acta, 298, 209–217, 1994.

Pitra, P., Kouamelan, A. N., Ballèvre, M., and Peucat, J.: Palaeoproterozoic high-pressure granulite overprint of the Archean continental crust: evidence for homogeneous crustal thickening (Man Rise, Ivory Coast), J. Metamorph. Geol., 28, 41–58, https://doi.org/10.1111/j.1525-1314.2009.00852, 2010.

Polat, A., and Kerrich, R.: Nd-isotope systematics of ~2.7 Ga adakites, magnesian andesites, and arc basalts, Superior Province: evidence for shallow crustal recy- cling at Archean subduction zones, Earth Planet. Sci. Lett., 202, 345–360, 2002.

Polat, A., Kerrich, R., and Wyman, D. A.: The late archean schreiber-hemlo and white river-dayohessarah greenstone belts, superior province: collages of oceanic plateaus, oceanic arcs, and subduction-accretion complexes, Tectonophysics, 289, 295–326, 1998.

Pons, J., Orléans, C., Oudin, J., and Valéro, V. V.: Kinematics of large syn-orogenic intrusions: example of the lower Proterozoic Saraya batholith (Eastern Senegal), Geol. Rundsch., 81, 473–486, 1992.

Pouclet, A., Doumbia, S., and Vidal, M.: Geodynamic setting of Birimian volcanism in central Ivory Coast (western Africa) and its place in the Paleoproterozoic evolution of the Man Shield, Bull. Soc. Géol. Fr., tome 177, 105–121, 2006.

Pouclet, A., Vidal, M., Delor, C., Siméon, Y., and Alric, G.: Le volcanisme birimien du nord-est de la Côte d'Ivoire, mise en évidence de deux phases volcanotectoniques distinctes dans l'évolution géodynamique du Paléoprotérozoïque, Bull. Soc. Géol. Fr., 167(4), 529-541, 1996.

Prinzhofer, L. A., Allegre, E., and Claude, J.: Stochastic melting of the marble cake mantle: evidence from local study of the east Pacific rise at 12 degree 50ÕN, Earth Planet. Sci. Lett., 92, 189–206, 1989.

https://doi.org/10.5194/egusphere-2025-814
Preprint. Discussion started: 11 April 2025

Ratomaharo, S., Demange, M., Fonteilles, M., and Treuil, M.: La série birrimienne de Perkoa (Burkina Faso). Géochimie et minéralogie. Interprétation lithostratigraphique. Conséquences sur l'interprétation géodynamique du Birrimien, C. R. Acad. Sci. Paris, 307, 2033–2040, 1988.

Regelous, M., Nui, Y., Wendt, J. I., Batiza, R., Grieg, A., and Collerson, K. D.: Variations in the geochemistry of magmatism on the East Pacific Rise at 10°30′N since 800 ka, Earth Planet. Sci. Lett., 168, 45–63, 1999.

Rospabé, M., Benoit, M., Ceuleneer, G., Hodel, F., and Kaczmarek, M. A.: Extreme geochemical variability through the dunitic transition zone of the Oman ophiolite: implications for melt/fluid-rock reactions at Moho level beneath oceanic spreading centers, Geochim. Cosmochim. Acta, 234, 1–23, https://doi.org/10.1016/j.gca.2018.05.012, 2018.

Ross, P. S., and Bédard, J. H.: Magmatic affinity of modern and ancient subalkaline volcanic rocks determined from trace-element discriminant diagrams, Can. J. Earth Sci., 46, 823–839, 2009.

Sakyi, P. A., Anum, S., Su, Ben-Xun, Nude, P. M., Su, Ben-Can, Asiedu, D. K., Nyame, F., and Kwayisi, D.: Geochemical and Sr-Nd isotopic records of Paleoproterozoic metavolcanics and mafic intrusive rocks from the West African Craton: Evidence for petrogenesis and tectonic setting, Geol. J., 53, 725–741, https://doi.org/10.1002/gj.2923, 2018.

Sangaré, A.: Les roches ultramafiques et mafiques Paléoprotérozoïques de la ceinture de roches vertes de Kadiolo (Mali). Pétrologie, évolution et ressources minérales associées, Mémoire de fin d'études, Master géosciences et ressources minérales, département des Sciences de la Terre, Université Sidi Mohamed Ben Abdellah, Maroc, 67 p, 2008.

Senyah, G. A., Dampare, S. B., and Asiedu, D. K.: Geochemistry and tectonic setting of the Paleoproterozoic metavolcanic rocks from the Chirano Gold District, Sefwi belt, Ghana, J. Afr. Earth Sci., 122, 32–46, https://doi.org/10.1016/j.jafrearsci.2015.07.022, 2016.

Sproule, R. A., Lesher, C. M., Ayer, J. A., Thurston, P. C., and Herzberg, C. T.: Spatial and temporal variations in the geochemistry of komatiites and komatiitic basalts in the Abitibi greenstone belt, Precambrian Res., 115, 153–186, 2002.

Stern, R. J., and Bibee, L. D.: Esmeralda bank: geochemistry of an active submarine volcano in the Mariana island arc, Contrib. Miner. Pet., 86, 159–169, 1984.

Stern, R. J., Lin, P. N., and Morris, J. D.: Enriched back-arc basin basalts from the northern Mariana trough: implications for the magmatic evolution of back-arc basins, Earth Planet. Sci. Lett., 100, 210–225, 1990.

Stern, R. J., Morris, J., Bloomer, S. H., and Hawkins, J. W.: The source of the subduction component in convergent margin magmas: Trace element and radiogenic isotope evidence from Eocene boninites, Mariana forearc, Geochim. Cosmochim. Acta, 55, 1467–1481, 1991.

Stolper, E., and Newman, S.: The role of water in the petrogenesis of Mariana trough magmas, Earth Planet. Sci. Lett., 121, 293–325, 1994.

Sun, S. S., and McDonough, W. F.: Chemical and isotopic systematics of oceanic basalts: implications for mantle composition and processes, Geol. Soc. Lond. Spec. Publ., 42, 313–345, https://doi.org/10.1144/GSL.SP.1989.042.01.19, 1989.

Sylvester, P. J., and Attoh, K.: Lithostratigraphy and composition of 2.1 Ga greenstone belts of the West African Craton and their bearing on crustal evolution and Archean-Proterozoic boundary, J. Geol., 100, 377–393, 1992.

https://doi.org/10.5194/egusphere-2025-814
Preprint. Discussion started: 11 April 2025

Theveniaut, H., Ndiaye, P.., Buscail, F., Coueffe, R., Delor, C., Fullgraf, T., and Goujou, J. C.: Notice explicative de la carte géologique du Sénégal oriental à 1/500000. Ministère des Mines, de l'industrie de l'agro- industrie et des PME, DMG, Dakar, 120 p, 2010.

Thiéblemont, D., Liégeois, J. P., Fernandez-Alonso, M., Ouabadi, A., Le Gall, B., Maury, R., Jalludin, M., Vidal, M., Ouattara Gbélé, C., Tchaméni, R., Michard, A., Nehlig, P., Rossi, P., and Chêne, F.: Geological map of Africa at 1:10M scale, CGMW-BRGM, 2016.

Tomlinson, K. Y., and Condie, K. C.: Archean mantle plumes: evidence from greenstone belt geochemistry, Geol. Soc. Am. Spec. Pap., 353, 341–357, 2001.

Velásquez, G., Béziat, D., Salvi, S., Tosiani, T., and Debat, P.: First occurrence of Paleoproterozoic oceanic plateau in the Guiana Shield: The gold-bearing El Callao Formation, Venezuela, Precambrian Res., 186, 181–192, https://doi.org/10.1016/j.precamres.2011.01.016, 2011.

Vidal, M., and Alric, G.: The Palaeoproterozoic (Birimian) of Haute-Comoé in the West African craton, Ivory Coast: a transtensional back-arc basin, Precambrian Res., 65, 207–229, 1994.

Vidal, M., Delor, C., Pouclet, A., Siméon, Y., and Alric, G.: Evolution géodynamique de l'Afrique de l'Ouest entre 2.2 GA et 2 Ga: le style archéen des ceintures vertes et des ensembles sédimentaires Birimiens du Nord-Est de la Côte-d'Ivoire, Bull. Soc. Géol. Fr., No. 167, 1996.

Volpe, A. M., Macdougall, G. W., Lugmair, J. W., Hawkins, J. W., and Lonsdale, P.: Fine-scale isotopic variation in Mariana trough basalts: evidence for heterogeneity and a recycled component in back-arc basin mantle, Earth Planet. Sci. Lett., 100, 251–264, 1990.

Volpe, A. M., Macdougall, J. D., and Hawkins, J. W.: Mariana Trough Basalts (MTB): trace element and Sr-Nd isotopic evidence for mixing between MORB-like and arc-like melts, Earth Planet. Sci. Lett., 82, 241–254, 1987.

White, W. M., and Patchett, J.: Hf-Nd-Sr isotopes and incompatible element abundances in island arcs: implications for magma genesis and crust-mantle evolution, Earth Planet. Sci. Lett., 67, 167–185, 1984.

Winchester, J. A., and Floyd, P. A.: Geochemical discrimination of different magma series and their differenciation products using immobile elements, Chem. Geol., 20, 235–343, 1977.

Windley, B. F., Kusky, T., and Polat, A.: Onset of plate tectonics by the Eoarchean, Precambrian Res., 352, 105980. https://doi.org/10.1016/j.precamres.2020.105980, 2021.

Woodhead, J. D.: The origin of geochemical variation in Mariana lavas: a general model for petrogenesis in intra-oceanic arcs, J. Petrol., 29, 805–830, 1988.

Yokoyama, T., Makishima, A., and Nakamura, E.: Evaluation of the coprecipitation of incompatible trace elements with fluoride during silicate rock dissolution by acid digestion, Chem. Geol., 157, 175–187, 1999.

Zonou, S.: Les formations leptino-amphibolitiques et le complexe volcanique et volcano-sédimentaire du Protérozoïque inférieur de Bouroum-nord (Burkina-Faso, Afrique de l'Ouest). Etude pétrographique, géochimique, approche pétrogénétique et évolution géodynamique, Thèse Univ., Nancy 1, France, 294 p, 1987.